

## Article

# Synthesis and Activity of Ionic Antioxidant-Functionalized PAMAMs and PPIs Dendrimers

Katia Bacha <sup>1,2</sup>, Julien Estager <sup>3</sup>, Sylvie Brassart-Pasco <sup>4</sup>, Catherine Chemotti <sup>2</sup>, Antony E. Fernandes <sup>3</sup>, Jean-Pierre Mbakidi <sup>1</sup>, Magali Deleu <sup>2</sup> and Sandrine Bouquillon <sup>1,\*</sup>

<sup>1</sup> Molecular Chemistry Reims Institute UMR CNRS 7312, Reims Champagne-Ardenne University, Boîte n° 44, B.P. 1039, 51687 Reims, France

<sup>2</sup> Laboratory of Molecular Biophysics at Interfaces (LBMI), Gembloux Agro-Bio Tech-Liège University Passage des Déportés, 5030 Gembloux, Belgium

<sup>3</sup> Certech, Rue Jules Bordet, 45 Zone Industrielle C, 7180 Senefte, Belgium

<sup>4</sup> UMR CNRS/URCA 7369 (MEDyC), Reims Champagne Ardenne University, 51 Rue Cognacq Jay CS30018, 51095 Reims, France

\* Correspondence: sandrine.bouquillon@univ-reims.fr; Tel.: +33-(0)-3-26-91-89-73; Fax: +33-(0)-3-26-91-31-66

**Abstract:** For this study, new dendrimers were prepared from poly(propylene imine) (PPI) and polyamidoamine (PAMAM) dendrimers using an efficient acid-base reaction with various phenolic acids. The syntheses were also optimized in both microwave and microfluidic reactors. These ionic and hydrophilic dendrimers were fully characterized and showed excellent antioxidant properties. Their cytotoxic properties have been also determined in the case of fibroblast dermal cells.

**Keywords:** dendrimers; phenolic acids; antioxidant; microwave; flow chemistry



**Citation:** Bacha, K.; Estager, J.; Brassart-Pasco, S.; Chemotti, C.; Fernandes, A.E.; Mbakidi, J.-P.; Deleu, M.; Bouquillon, S. Synthesis and Activity of Ionic Antioxidant-Functionalized PAMAMs and PPIs Dendrimers. *Polymers* **2022**, *14*, 3513. <https://doi.org/10.3390/polym14173513>

Academic Editor: Craig A. Bell

Received: 21 July 2022

Accepted: 23 August 2022

Published: 27 August 2022

**Publisher's Note:** MDPI stays neutral with regard to jurisdictional claims in published maps and institutional affiliations.



**Copyright:** © 2022 by the authors. Licensee MDPI, Basel, Switzerland. This article is an open access article distributed under the terms and conditions of the Creative Commons Attribution (CC BY) license (<https://creativecommons.org/licenses/by/4.0/>).

## 1. Introduction

Dendrimers are hyperbranched macromolecules having, in general, a three-dimensional, monodisperse and globular structure, most of the time with a perfect tree-like structure [1,2]. They are largely studied mainly for their encapsulation capacity, particularly in the biomedical field [3]. Recently, Kaur et al. presented an interesting review concerning a comparative study of poly(propyleneimine) (PPI) and polyamidoamine (PAMAM) dendrimers, some of the most-used dendrimers [4]. In recent years, we have developed various dendrimers containing biobased moieties to make these compounds more eco-compatible. These have been used in catalysis, medical imaging and depollution [5–8]. The present study is devoted to the preparation of new ionic dendrimers that present, moreover, antioxidant properties. Indeed, these new macromolecules are designed for original use as carriers in cosmetics; the encapsulation will limit active compound degradation, their ionic character will improve their solubility in compatible solvents for cosmetics, and their antioxidant power will protect the macromolecules themselves and reinforce their beneficial encapsulating role. To our knowledge, no dendrimers presenting both ionic and antioxidant characteristics have yet been described in the literature.

However, the synthesis of ionic dendrimers has previously been described in the literature, for example, dendronized pyridinium units surrounded by a shell of carboxylic acids [8] or water-soluble polyanionic dendrimers, presenting great potential applications as antiviral drugs [9]. Ionic dendrimers have also been used as a base for polyamide membranes for ion separation [10] or electrolytes for LiS batteries [11]. Their use in the form of liquid crystals has also been investigated alongside, for instance, ionic dendrimers as poly(ethylene imine) polymers functionalized by oxadiazole [12,13] or fluorinated and perhydrogenated chains [14].

Antioxidant dendrimers have been prepared using two approaches. The first approach consists of the synthesis of new dendritic structures presenting antioxidant properties; the

second approach is based on the capacity of existing dendrimers to encapsulate antioxidant compounds. In the first approach, phenols could be used as the starting material of choice to build antioxidant moieties. Indeed, dendritic polyphenols have been prepared and evaluated as antioxidant compounds [15–17], for use either coupled with cis-platin as an anticancer agent [18] or mostly in polyolefin to avoid the peroxidation of the olefins [19,20]. Carbosilane, when functionalized by polyphenols, also presents antioxidant, antibacterial and anticancer properties [21,22]. The decoration of PAMAM [23–25], glycodendrimers [26] or original dendrimers (triazole-bridged, hyperbranched polyurethanes, with an enone or anthraquinone or melamine core) [27–32]; these are partnered with specific entities, such as polyphenols, Meldrum's acid derivatives, carbazole, fluorescein or Rhodamine that have also led to new dendritic molecules presenting, among others, good antioxidant properties. Decorated peptide dendrimers have also presented excellent antioxidant properties [33], as well as original radical dendrimers [34].

The second approach for preparing antioxidant dendrimers is related to their capacity to encapsulate various types of compounds (organic or organometallic compounds, salts and nanoparticles). Indeed, dendrimers or dendrimer nanoparticles have largely been used in therapeutic domains. Curcumin [35,36], gold nanoparticles [37], astragaloside [38], cis-platin [39] and sinomenine or minocycline [40,41] were encapsulated in different dendrimers (PAMAM, modified PAMAM and carbosilane dendrimers), leading to controlled release for targeted therapy. Gallic acid-modified PAMAM dendrimers were also explored as novel strategies to fight the chemoresistance of tumor cells [42,43]. These last compounds were also used as devices for the long-term preservation of essential oils [44]. Dendrimers such as PAMAM [45], chitosan-poly(amidoamine) dendrimer [46], or dendrimer-like glucan [47] were also employed to stabilize antioxidants, such as carotene [47], coenzyme Q10 [48], resveratrol [49] or polyphenols [50], showing excellent antioxidant activities.

In the present study, we will describe the preparation of new ionic dendritic structures from a simple acid-base reaction between PAMAMs or PPIs and phenolic acids without a coupling agent. The nitrogen-based moieties are cationic, and the anion is the carboxylate form of the phenolic acids. The antioxidant properties are carried by ionic species; the electrostatic linkage can enhance the compounds' solubility in water and may influence the cytotoxic properties of the dendritic structures. These compounds have been synthesized in a swift and efficient way, using either microwave or microfluidic reactors. Both techniques—which are strongly linked to sustainable chemistry [23,51,52]—are known to significantly accelerate the reaction kinetics, taking advantage of either very fast and homogeneous heating through dielectric loss, in the case of microwaves (MW) [53], or from very efficient mass and heat transfer, in the case of flow chemistry [54]. These techniques have been used for the synthesis of many chemicals, including, for example, active pharmaceutical ingredients [55] or biobased compounds [56,57].

## 2. Results and Discussion

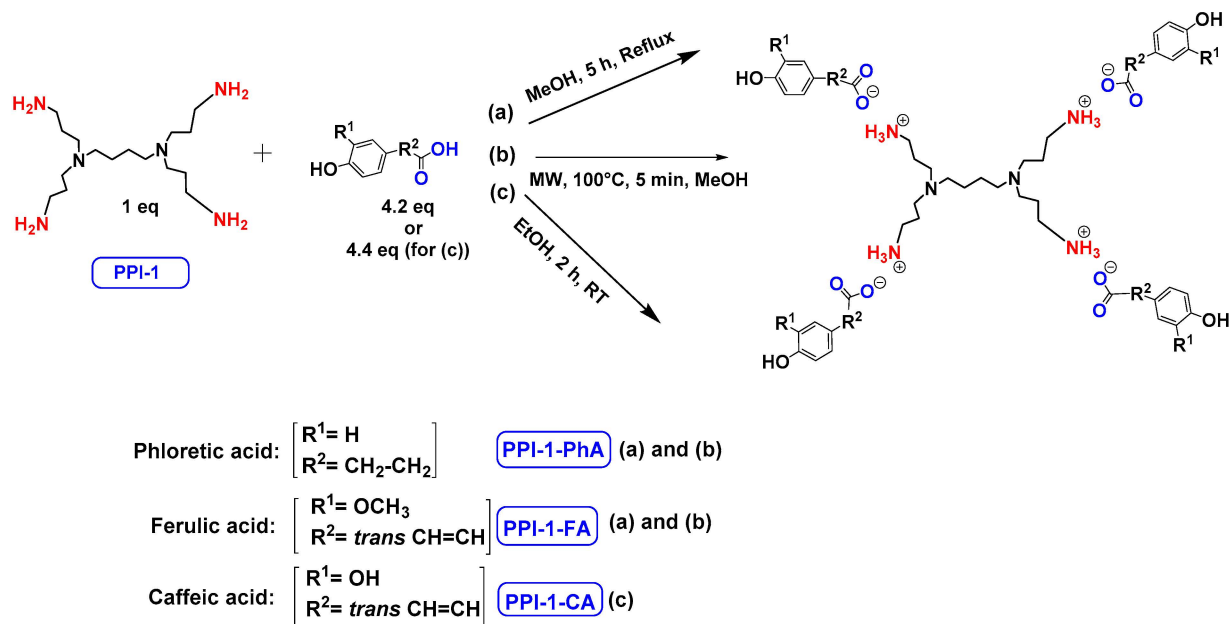
### 2.1. Synthesis of the Ionic Dendrimers

In this study, oligomers synthesized from 3 generations of PPI dendrimers and 3 biobased phenolic acids (phloretic, ferulic and caffeic acids) were first targeted.

Poly(propylene imine) (PPI) dendrimers [58] are also known as DAB-Am-x dendrimers (DAB, for the diaminobutane core, and  $x = 4, 8, \text{ or } 16$ , for the number of primary amine end groups associated with generations 1, 2, or 3, respectively). Phloretic acid (PhA), found, among others, in olives [59] or in the bran extracts of traditional rice cultivars [60], was used in a recent application as a biocompatibilizer for immiscible polymer blends [61]. Ferulic acid (FA) is widely present in plants in either its free or conjugated forms and is well known for many various applications in the medical field, thanks to its bioactivity, for the treatment of cancer, diabetes, and lung and cardiovascular diseases [62]. Ferulic acid has a protective role for the main skin structures (keratinocytes, fibroblasts, collagen and elastin); it inhibits melanogenesis, enhances angiogenesis, and accelerates wound healing [63]. Caffeic acid (CA), extracted from specific plants' biomass, is a dietary polyphenol.

nol that is also considered a promising drug candidate, thanks to its efficiency against inflammatory, neurodegenerative, oncologic and metabolic disorders [64,65]. Caffeic acid also presents a photoprotective effect in irradiated lymphocytes [66] and could act as a potent chemopreventive agent against skin cancer [67].

The synthesis of these new families of functionalized PPIs with the phenolic acid derivatives, PPIs-PhA, PPIs-FA and PPIs-CA, was realized by an acid-base reaction of commercial PPIs with ferulic acid, phloretic acid and caffeic acid, respectively, in methanol or ethanol under various conditions (Scheme 1, Table 1). This reaction has the advantage of not requiring coupling agents when compared to the traditional amidation reaction, for instance.

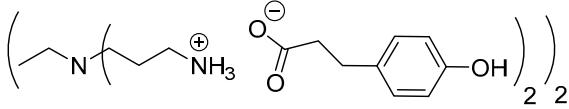
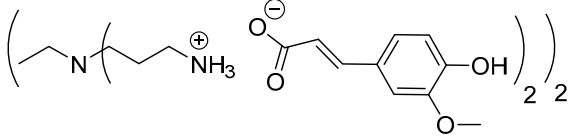
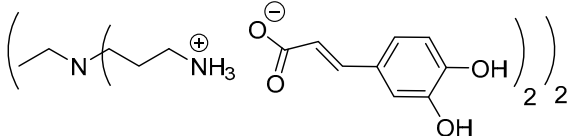
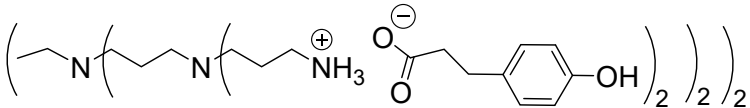
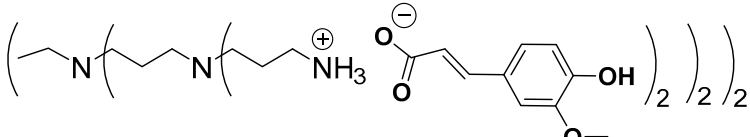
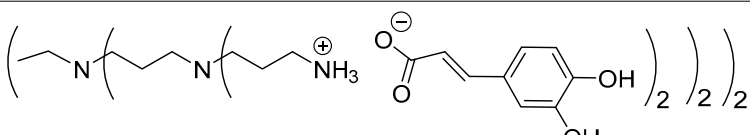
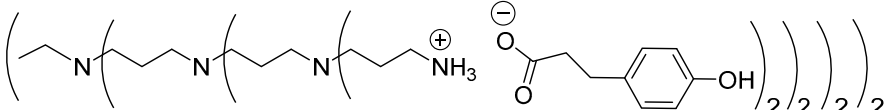
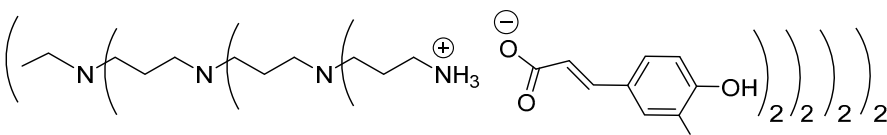
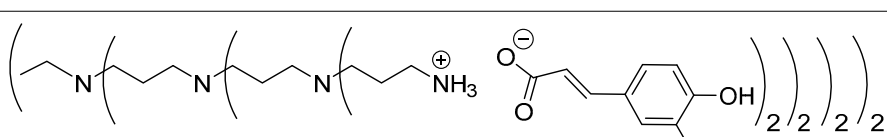


**Scheme 1.** The ionic functionalization of PPIs with phloretic, ferulic and caffeic acids.

The first-generation dendrimers, PPI-1-PhA and PPI-1-FA, were obtained by a reaction between the terminal primary amines of first-generation PPI (PPI-1) with phloretic acid or ferulic acid, respectively, in refluxing methanol for 5 h (Scheme 1(a)). Reflux was necessary to obtain higher yields in lower times. This reaction was confirmed by  $^1H$  NMR, focusing on the chemical shift of the protons of the  $CH_2$  groups linked to the terminal primary amine functions (2.67 ppm for PPI-1, 2.91 ppm and 2.98 ppm, respectively, for PPI-1-PhA and PPI-1-FA in  $CD_3OD$ ) and by  $^{13}C$  NMR analyses, focusing on the chemical shift of the carbon from the carbonyl group (176.3 and 169.6 ppm, respectively), for phloretic acid and ferulic acid; 180.4 and 174.7 ppm, respectively, for PPI-1-PhA and PPI-1-FA in  $CD_3OD$  (see Section 3.1). These shifts toward lower fields are consistent with salt formation between the amines and carboxylic acids [68].

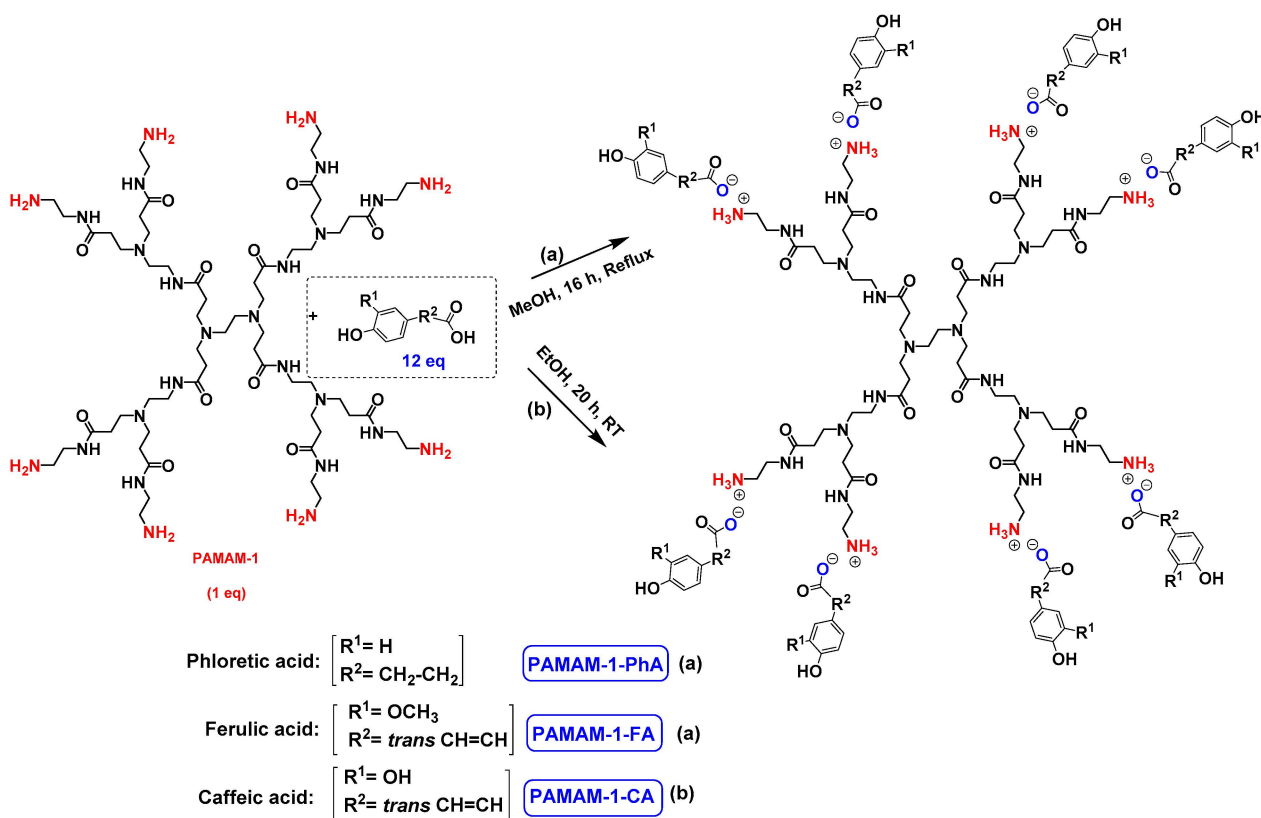
Two-dimensional NMR analyses were also performed to prove that no formation of amide functions occurred instead of forming ionic compounds. Next, the disappearance of the strong  $\nu(CO)$  bands of phloretic acid and ferulic acid using IR ( $1699\ cm^{-1}$  and  $1689\ cm^{-1}$ , respectively), as well as the two new  $\nu(CO)$  bands of ionized acids at  $1540\ cm^{-1}$  and  $1396\ cm^{-1}$  for PPI-1-PhA and at  $1539\ cm^{-1}$  and  $1394\ cm^{-1}$  for PPI-1-FA, confirmed the formation of the ionic dendrimers [68]. The purification of PPI-1-PhA and PPI-1-FA was performed by solubilizing the crude mixture in water, followed by extraction with ethyl acetate. Similarly, the second and third generations of PPIs-PhA and PPIs-FA were obtained in quantitative yields.

Table 1. Ionic PPI-derived dendrimers.

Starting Dendrimers	Ionic Dendrimers/Yields
PPI-1	 <p>PPI-1-PhA &gt; 97%</p>
	 <p>PPI-1-FA &gt; 97%</p>
	 <p>PPI-1-CA 90%</p>
PPI-2	 <p>PPI-2-PhA &gt; 97%</p>
	 <p>PPI-2-FA &gt; 97%</p>
	 <p>PPI-2-CA 90%</p>
PPI-3	 <p>PPI-3-PhA &gt; 97%</p>
	 <p>PPI-3-FA &gt; 97%</p>
	 <p>PPI-3-CA 92%</p>

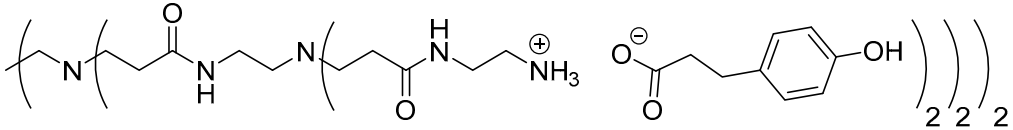
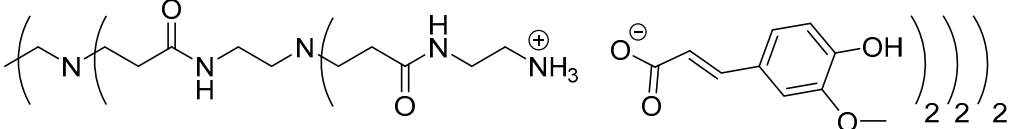
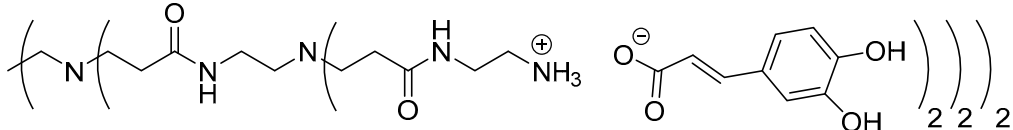
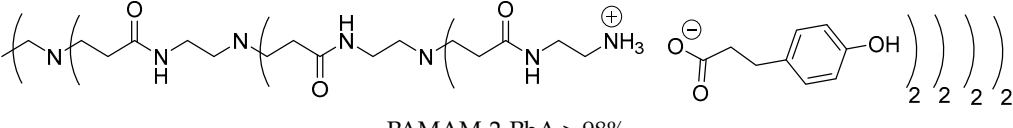
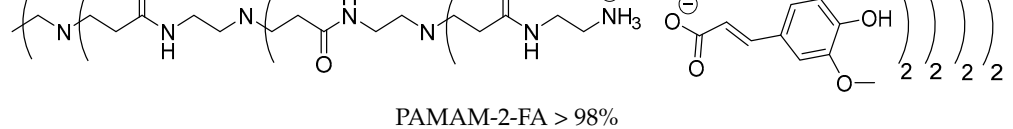
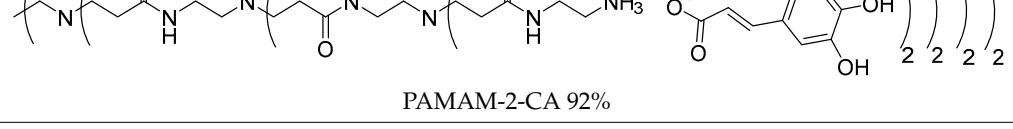
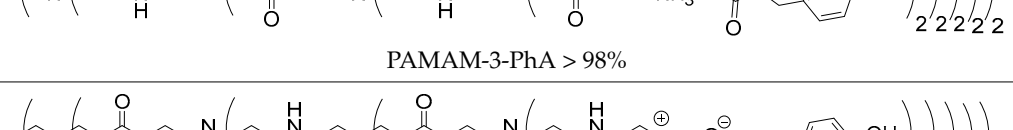
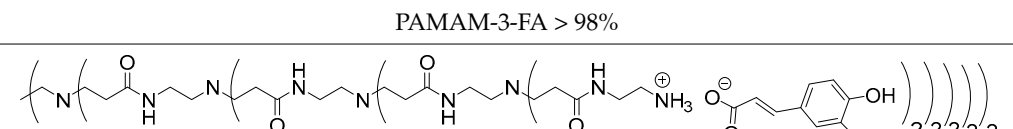
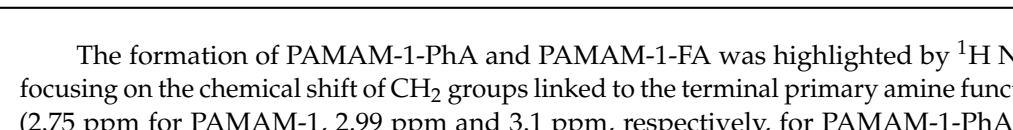
Concerning the preparation of PPIs-CA, the conditions were adapted because the mixture of the two reagents (PPI and caffeic acid) in methanol precipitates as a brown wax. First-generation PPI-1-CA was, therefore, obtained by reacting the terminal primary amines of a PPI-1 with caffeic acid in ethanol at room temperature under orbital stirring (280 rpm), with the dropwise addition of the caffeic acid ethanolic solution (Scheme 1 (c)). The formation of PPI-1-CA was investigated by NMR, focusing firstly on the chemical shift of the H5 protons (see Section 3.1) corresponding to the CH<sub>2</sub> groups that are linked to the terminal primary amine functions (2.53 ppm for PPI-1 and 2.73 ppm for PPI-1-CA in (CD<sub>3</sub>)<sub>2</sub>SO), and secondly on the chemical shift of the C6 carbons (see Section 3.1) corresponding to the carbonyl groups (168.4 ppm for caffeic acid and 171.6 ppm for PPI-1-CA in (CD<sub>3</sub>)<sub>2</sub>SO). IR analyses confirmed the nature of the product through the disappearance of the strong νCO band of caffeic acid at 1640 cm<sup>-1</sup> and the appearance of two νCO bands of ionized acid around 1507 cm<sup>-1</sup> and 1372 cm<sup>-1</sup> for PPI-1-CA, as previously described [68]. The purification of PPI-1-CA was finally performed by washing the resulting precipitate with ethanol, followed by centrifugation. The second and third generations (PPI-2-CA and PPI-3-CA) were prepared following the same process and were obtained at yields above 90%.

The synthesis of PAMAM dendrimers functionalized with phenolic acids, PAMAMs-PhA, PAMAMs-FA and PAMAMs-CA, were performed in the same way via the acid-base reaction of commercial PAMAMs with ferulic, phloretic and caffeic acids, respectively, in methanol or ethanol (Scheme 2, Table 2). However, it was necessary to increase the number of equivalents of phenolic acid (up to 1.5 equiv. per NH<sub>2</sub>) and the reaction time (up to 16 or 20 h), probably because of the steric hindrance caused by the morphology of the PAMAMs, which prevents the insertion of phenolic acids and the formation of ionic bonds.



Scheme 2. Ionic functionalization of PAMAMs with phloretic, ferulic and caffeic acids.

Table 2. Ionic PAMAM-derived dendrimers.

Starting Dendrimers	Ionic Dendrimers/Yields
PAMAM-1	 <p>PAMAM-1-PhA &gt; 98%</p>
	 <p>PAMAM-1-FA &gt; 98%</p>
	 <p>PAMAM-1-CA &gt; 99%</p>
PAMAM-2	 <p>PAMAM-2-PhA &gt; 98%</p>
	 <p>PAMAM-2-FA &gt; 98%</p>
	 <p>PAMAM-2-CA 92%</p>
PAMAM-3	 <p>PAMAM-3-PhA &gt; 98%</p>
	 <p>PAMAM-3-FA &gt; 98%</p>
	 <p>PAMAM-3-CA &gt; 99%</p>

The formation of PAMAM-1-PhA and PAMAM-1-FA was highlighted by  $^1\text{H}$  NMR, focusing on the chemical shift of  $\text{CH}_2$  groups linked to the terminal primary amine functions (2.75 ppm for PAMAM-1, 2.99 ppm and 3.1 ppm, respectively, for PAMAM-1-PhA and PAMAM-1-FA in  $\text{CD}_3\text{OD}$ ). The  $^{13}\text{C}$  NMR also shows a chemical shift of the carbonyl carbons (176.3 ppm and 169.6 ppm, respectively, for phloretic acid and ferulic acid; 180.6 ppm and

174.6 ppm, respectively, for PAMAM-1-PhA and PAMAM-1-FA in CD<sub>3</sub>OD (see Section 3.1)). Following the same procedure, the second and third generations of PAMAMs-PhA and PAMAMs-FA were prepared, with yields above 90%.

Once again, solubility issues occurred with caffeic acid; the formation of the first-generation PAMAM-1-CA was performed by reacting PAMAM-1 with caffeic acid in ethanol (instead of methanol) at room temperature, adding the caffeic acid solution dropwise (Scheme 2 (b)). In this case, no heating of the medium was required to obtain good yields. The formation of PAMAM-1-CA was followed by <sup>1</sup>H and <sup>13</sup>C NMR, focusing on the chemical shift of the H11 protons corresponding to the CH<sub>2</sub> groups linked to the terminal primary amine functions (see Section 3.1) (2.55 ppm for PAMAM-1 and 2.78 ppm for PAMAM-1-CA in (CD<sub>3</sub>)<sub>2</sub>SO) and on the chemical shift of the C12 carbons corresponding to the carbonyl function (see Section 3.1) (168.4 ppm for caffeic acid, 172.5 ppm for PAMAM-1-CA in (CD<sub>3</sub>)<sub>2</sub>SO). The disappearance of a strong νCO band of caffeic acid, observed in IR at 1640 cm<sup>-1</sup>, and the appearance of two νCO bands of ionized acid around 1522 at 1580 cm<sup>-1</sup> and 1376 cm<sup>-1</sup> for PAMAM-1-CA, confirm the formation of the ionic substrates. The second and third generations (PAMAM-2-CA and PAMAM-3-CA) were prepared similarly, with good yields of higher than 99%.

## 2.2. Synthesis in MW and Microfluidic Reactors

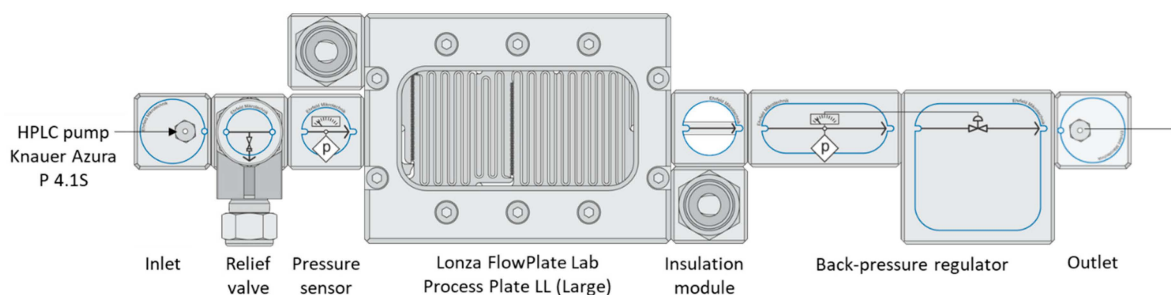
The feasibility of the reaction using microwave irradiation was demonstrated with PPI dendrimers, when the different syntheses were then optimized. Taking advantage of the fast and efficient heating induced by microwave organic synthesis, the formation of PPIs-PhA, PPIs-FA and PPIs-CA could be achieved in only 5 min at 100 °C (Scheme 1 (b)) with very high isolated yields. The different results obtained are summarized in Table 3.

**Table 3.** Synthesis of ionic dendrimers in MW and flow reactors.

Ionic Dendrimer	Residence Time (Min.)	Temp. (°C)	Pressure (Bar)	Yields (%) (MW)	Yields (%) (Flow Reactors)
PPI-1-PhA	5	100	3.5	>97	>97
PPI-1-FA	5	100	3.5	>97	94
PPI-2-PhA	5	100	3.5	>97	>97
PPI-2-FA	5	100	3.5	>97	86
PPI-3-FA	5	100	3.5	>97	71
PAMAM-1-PhA	5	100	3.5	- <sup>a</sup>	98
PAMAM-1-FA	5	100	3.5	- <sup>a</sup>	82

<sup>a</sup> The microwave-assisted reaction was not performed with PAMAM dendrimers.

Flow synthesis in a mesofluidic reactor was also investigated in the search for a process that is both time/energy-efficient and easily scalable. Considering the different results obtained in the batches, the feasibility of the methodology was tested using a commercial flow reactor of 1.2 mL (Lonza FlowPlate Lab used on an MMRS flow reactor from Ehrfeld). If compared to microwave irradiation technology, the use of a microfluidic device can lead to an easier scale-up, either by scaling up, sizing up or numbering up [69]. For this study, the system was designed to enable the continuous supply of a mixture containing either a PPI or a PAMAM precursor and carboxylic acid (PhA or FA) in methanol. The use of a back-pressure regulator (BPR) enabled us to work above the boiling point of the solvent, thereby accelerating the overall process. It is noteworthy that caffeic acid was not tested, as the different salts obtained tended to precipitate, leading to clogging of the system. The set-up of the system used for these syntheses is presented in Scheme 3 below.



**Scheme 3.** The setup used for the flow synthesis of antioxidant ionic dendrimers, based on various PPI and PAMAM.

The high heat transfer provided by the microfluidic device, as well as this high temperature (100–120 °C) to perform the reaction within 5 min, as observed when microwave irradiation was used. This microwave/flow similarity is common and has been theorized to be the *microwave-to-flow paradigm* [70]. The different products were isolated as described in Section 3.1; in each case, yellowish solids were obtained, their purity being assessed by  $^1\text{H}$  NMR. The different yields, as well as the experimental conditions, are summarized in Table 4 below. Each test was duplicated.

**Table 4.** Antioxidant activity of ionic dendrimers, determined as  $\text{IC}_{50}$ .

Entry	Samples	$\text{IC}_{50}$ ( $\mu\text{mol/L}$ )	Standard Deviation	$\text{IC}_{50}$ ( $\mu\text{mol/L}$ ) per Antioxidant Unit	Ratio $\text{IC}_{50}$ ( $\mu\text{mol/L}$ ) per Antioxidant Unit/ $\text{IC}_{50}$ ( $\mu\text{mol/L}$ ) (%)
1	Vitamin C	62.0	$\pm 1.4$	62.0	100
2	Ferulic acid	270.0	$\pm 2.4$	270.0	100
3	PPI-1-FA (4 FA units)	30.0	$\pm 1.8$	120	44
4	PPI-2-FA (8 FA units)	17.0	$\pm 2.1$	136	50
5	PPI-3-FA (16 FA units)	10.0	$\pm 2.6$	160	60
6	PAMAM-1-FA (8 FA units)	22.0	$\pm 2.0$	176	65
7	PAMAM-2-FA (16 FA units)	8.60	$\pm 1.3$	137.6	50
8	PAMAM-3-FA (32 FA units)	4.80	$\pm 0.8$	153.6	57
9	Caffeic acid	13.0	$\pm 1.2$	13	100
10	PPI-1-CA (4 CA units)	10.1	$\pm 1.3$	40.4	300
11	PPI-2-CA (8 CA units)	7.5	$\pm 1.0$	60	400
12	PPI-3-CA (16 CA units)	3.5	$\pm 1.1$	56	400
13	PAMAM-1-CA (8 CA units)	5.4	$\pm 1.1$	43.2	300
14	PAMAM-2-CA (16 CA units)	1.8	$\pm 0.9$	28.8	200
15	PAMAM-3-CA (32 CA units)	1.0	$\pm 0.4$	32	200
16	PAMAM-3-PhA	480.0	$\pm 4.3$	-	-

### 2.3. Determination of the Antioxidant Properties

The antioxidant capacity of the ionic dendrimers was evaluated by measuring their ability to inhibit a DPPH radical. Several spectroscopic methods are described in the literature to measure the inhibition of the DPPH radical by an antioxidant [71], while UV-visible spectroscopy was used in another work [72]. The trapping of DPPH radicals by ionic dendrimers led to a color change from purple to yellow, relative to an  $\text{H}\bullet$  transfer. This color change implies a decrease in the absorbance (A) of the DPPH radical at 515 nm. The results are expressed as a percentage of inhibition (I %), calculated according to the following formula:

$$I\% = \frac{A(\text{DPPH}) - A(\text{DPPH} + \text{antioxidant})}{A(\text{DPPH})} \times 100$$

where  $A(\text{DPPH})$  is the absorbance of DPPH and  $A(\text{DPPH} + \text{antioxidant})$  is the absorbance of the mixture of DPPH and substrate at 515 nm.

The evaluation of the antioxidant power was determined for 5 families of dendrimers, namely, PPIs-FA, PPIs-CA, PAMAMs-FA, PAMAMs-CA and PAMAMs-PhA and caffeic and ferulic acids, with ascorbic acid (vitamin C) used as the positive control [73].

The effect of dendrimer concentration is shown in Figures 1 and 2. From these curves, the  $\text{IC}_{50}$  of each dendrimer, i.e., the concentration of an antioxidant to inhibit 50 percent of free radicals at a given concentration, was graphically determined (Table 4). The  $\text{IC}_{50}$  curves in mg/L are given in the Supplementary Materials.

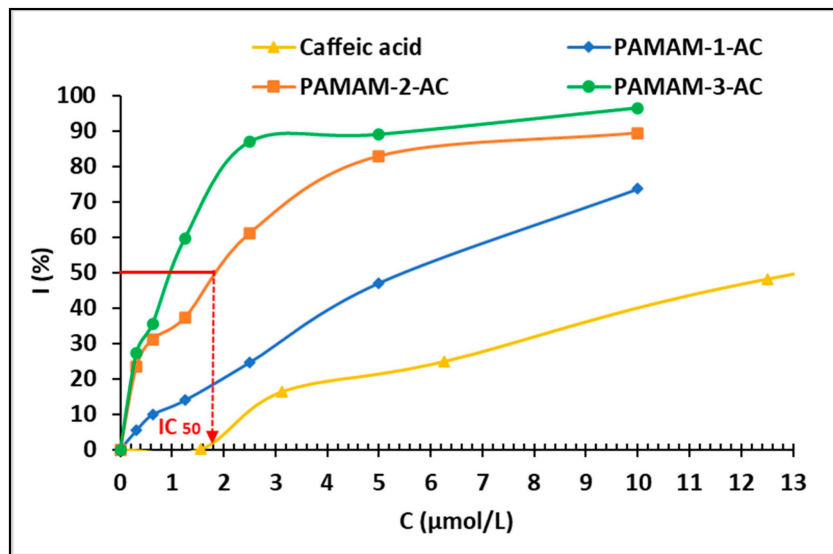


Figure 1. The inhibition of DPPH (300 μM) by caffeic acid-derived PAMAM dendrimers.

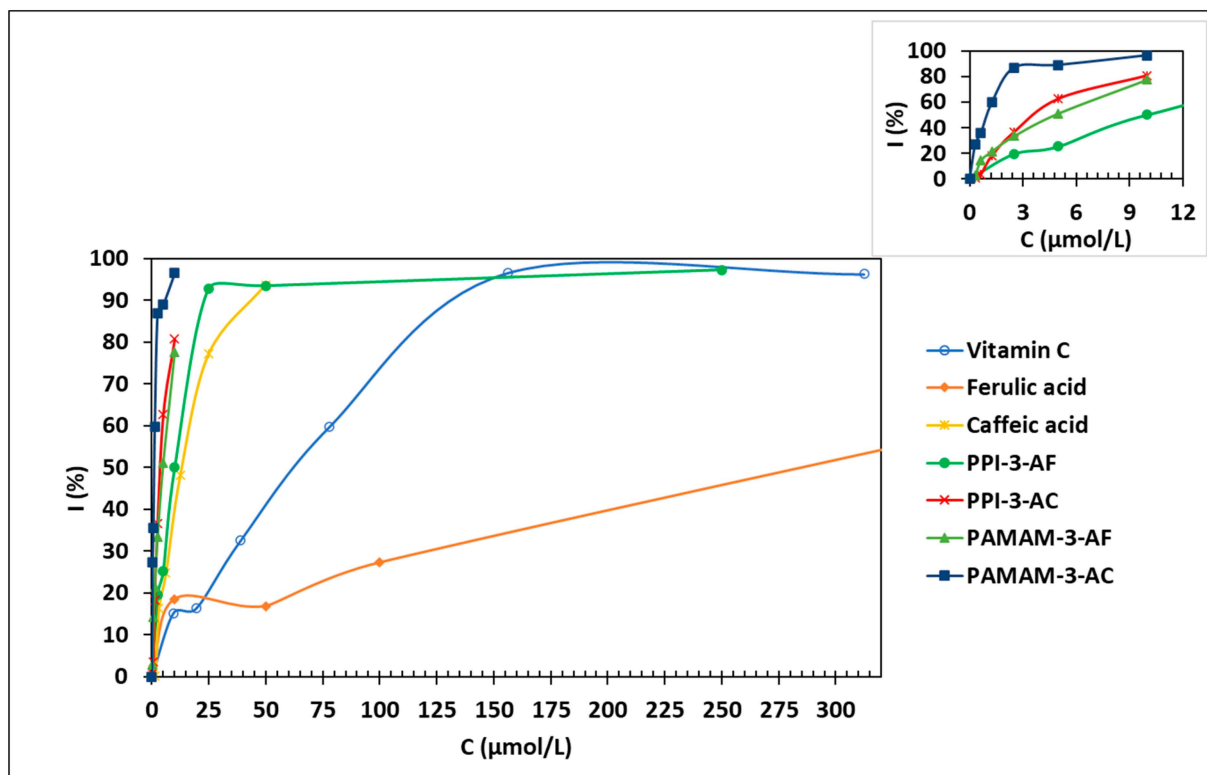


Figure 2. The inhibition of DPPH (300 μM) by ionic antioxidant dendrimers.

These results show that antioxidant activity depends on the generation of the dendrimer (Table 4, entries 3–5, 6–8, 10–12 and 13–15). Indeed, for higher generations, more phenolic carboxylates are present, leading to higher antioxidant molar activities (Figure 1).

Dendrimers derived from PAMAMs exhibit higher antioxidant activity, compared to PPI-based ones for the same generation. Once again, this observation can be ascribed to a larger number of phenolic carboxylates for PAMAM, compared to PPI (a ratio of 2) for a given generation. The level of antioxidant activity also depends on the nature of the antioxidant and is mainly linked to the number of hydroxyl functions present in the structures. Indeed, the best antioxidant activities are obtained for the caffeic acid derivatives, PPI-3-CA and PAMAM3-CA, where the  $IC_{50}$  values are  $3.5 \pm 1.1 \mu\text{mol/L}$  and  $1.0 \pm 0.4 \mu\text{mol/L}$  (Figure 2), respectively, while the antioxidant activities of the ferulic acid derivatives are lower (Table 4, entries 3–8). Furthermore, it is important to mention that caffeic acid not only possesses better antioxidant properties but is also more stable than vitamin C [74,75].

As the dendrimers contain several antioxidant units, a ratio between ionic dendrimers and the corresponding acid was calculated (Table 4). Thus, we observed that ionic PPIs or PAMAM ferulates are more strongly antioxidant than pure ferulic acid, while in the case of caffeic acid, the latter remains the most antioxidant. This could be explained by a close interaction between OH groups of CA from the different arms of the dendrimer and/or OH and NH from the dendrimer itself; the solubility of the complex dendrimer/CA could also explain the difference in antioxidant activity.

In conclusion, dendrimers show good or even very good antioxidant activities and have the characteristic of being able to encapsulate various compounds of interest, particularly in the field of cosmetics.

For all ferulic and caffeic dendrimers, absorbance measurements at 515 nm were recorded every 90 s for 45 min and revealed no significant variation in absorbance as a function of time after 5 min of reaction with DPPH, meaning that their antioxidant activities appear quickly and are stable. On the other hand, a significant variation in the absorbance is observed for PAMAM-3-PhA with the passage of time (Figure 3). Indeed, after 5 min, the percentage of inhibition of 300  $\mu\text{M}$  DPPH by PAMAM-3-PhA at 5 mM concentration is 45%, while it increases to more than 90% for  $t = 18$  min (Figure 3). For this reaction time, the  $IC_{50}$  of PAMAM-3-PhA is 480  $\mu\text{mol/L}$ . The antioxidant power of the latter is, thus, less important and takes more time to set up, compared to the other families of dendrimers derived from ferulic and caffeic acids.

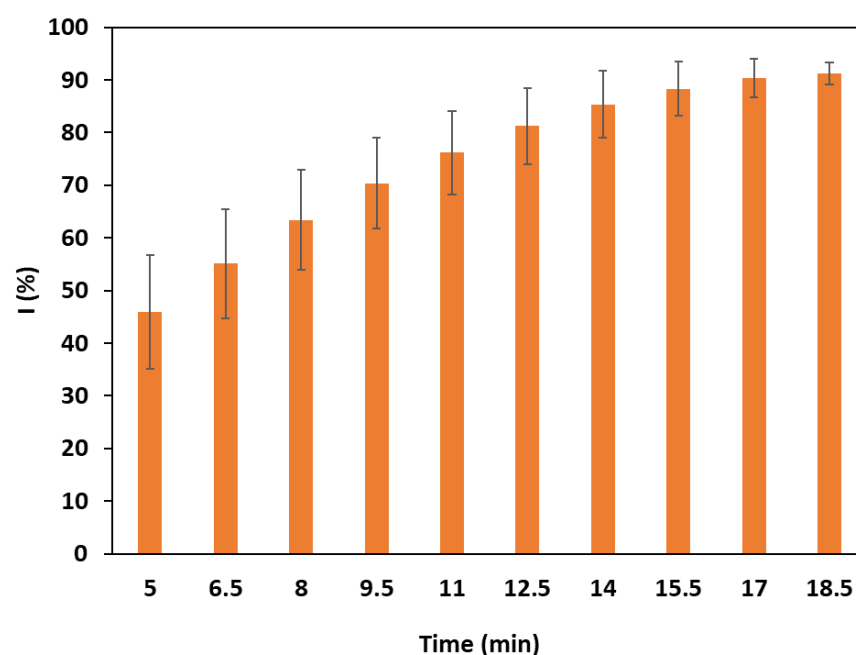
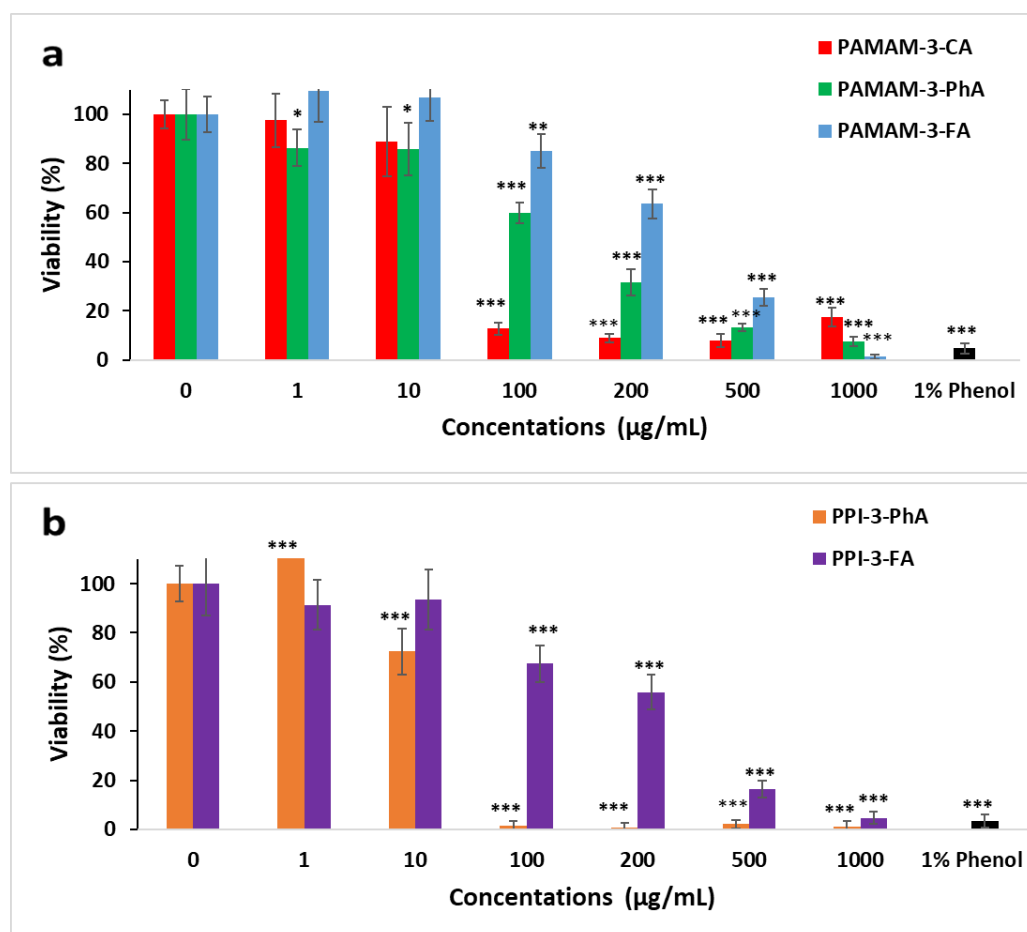


Figure 3. The inhibition of DPPH (300  $\mu\text{M}$ ) by PAMAM-3-PhA (5 mM).

#### 2.4. Determination of Cytotoxic Properties

Based on the results of the toxicity tests performed on GD-PPI-4 and GD-PAMAM-3 dendrimers on human MRC5 fibroblasts [5,76], the cytotoxicity of five dendrimers, PPI-3-FA, PPI-3-PhA, PAMAM-3-FA, PAMAM-3-PhA, and PAMAM-3-CA was tested on human dermal fibroblasts using two methods, the WST1 assay and cell staining with crystal violet, as described in Section 3.1. Dermal fibroblasts were incubated for 48 h in the presence of increasing concentrations of each dendrimer, while the number of living cells was established by a WST-1 reduction test. Cell toxicity with all dendrimers was observed as soon as a concentration of 100  $\mu\text{g}/\text{mL}$  was reached, except in the case of PPI-3-PhA, where toxicity was observed at 10  $\mu\text{g}/\text{mL}$  (Figure 4a,b). At 100  $\mu\text{g}/\text{mL}$ , 80%, 67%, 60%, 13% and 2% of living cells were detected in the presence of PAMAM-3-FA, PPI-3-FA, PAMAM-3-PhA, PAMAM-3-CA and PPI-3-PhA, respectively. Above this concentration, cell viability decreased with an increase in concentration to about 2% at 1000  $\mu\text{g}/\text{mL}$  for all studied dendrimers. Dendrimers derived from ferulic acid remained less toxic than caffeic- and phloretic-derived ones, while the PPI-3-PhA dendrimer was the most toxic. Figure 5 shows the images of human dermal fibroblast cells in the presence of different dendrimers using an EVOS XL Core inverted microscope, whereby the cytotoxicity is well highlighted. Hence, at 100  $\mu\text{g}/\text{mL}$ , PAMAM-3-FA and PPI-3-FA could be used in cosmetics as encapsulating and antioxidant agents for active ingredients.



**Figure 4.** Cytotoxic effects of the phenolic acids (a) derived from PAMAM and (b) derived from PPI dendrimers on human dermal fibroblast cells, evaluated by a WST-1 assay (\*:  $p < 0.01$ , \*\*:  $p < 0.001$ , \*\*\*:  $p < 0.0001$ ).

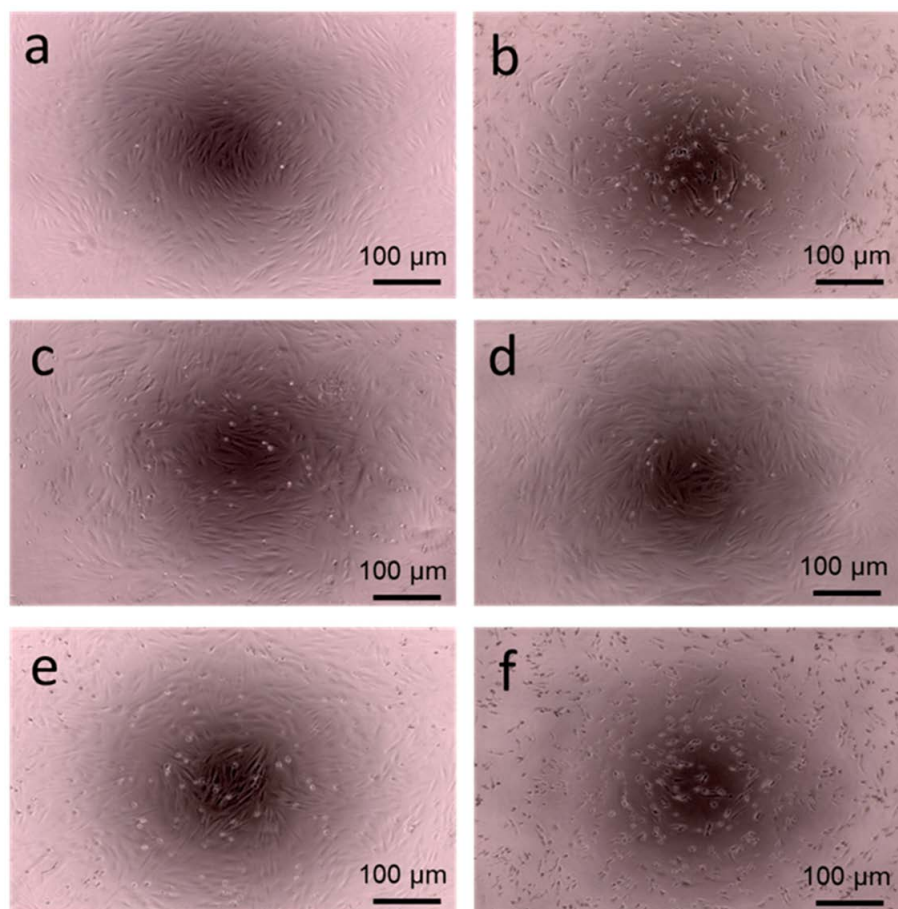


**Figure 5.** Cytotoxic effects of (b) PAMAM-3-CA, (c) PAMAM-3-FA, (d) PAMAM-3 PhA, (e) PPI-3-FA and (f) PPI-3-PhA at 100  $\mu\text{mol/L}$  on a human dermal fibroblast cell, compared with (a) a blank living cell. Cells were imaged using an EVOS XL Core inverted microscope ( $\times 10$  magnification).

### 3. Conclusions

In the present work, 18 new ionic dendrimers have been easily prepared from PPI and PAMAM dendrimers and 3 biobased phenolic acids through a classical acid basic procedure. These syntheses were optimized under microwave activation and then transferred to a continuous flow microreactor, leading to high yields within short reaction times. The ionic dendrimers present very interesting antioxidant activities, even being superior to that of vitamin C, which was taken as the reference substance. These antioxidant activities depend on both the nature of the dendrimer and the phenolic acid used. The best antioxidant activities are observed with dendrimers PAMAMs-1-3-FA and PAMAMs-1-3-CA, both of these being stable compounds. Hence, at 100  $\mu\text{g/mL}$ , PAMAM-3-FA and PPI-3-FA could be used in cosmetics as encapsulating and antioxidant agents for active ingredients. Studies of encapsulation of bioactive compounds are in progress and the synergy of the antioxidant power of the dendrimer and its encapsulation capacity are now under investigation.

#### 3.1. Experimental

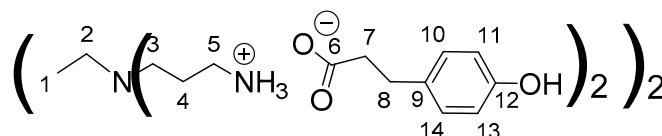
PPIs, PAMAMs, phloretic acid, ferulic acid, caffeic and solvent were purchased from traditional chemical suppliers and used without further purification. NMR spectra (d: doublet, t: triplet and qt: quintuplet) were recorded at 298 K at 500 MHz for  $^1\text{H}$  and 125 MHz for  $^{13}\text{C}$  on an Avance III Bruker spectrometer in  $\text{CD}_3\text{OD}$  or  $(\text{CD}_3)_2\text{SO}$ . IR spectra (S: strong) were recorded on a Perkin Elmer Spectrum Two. Elemental analyses (C, H, N) were realized on a Flash EA-1112 Series. The microwave-assisted syntheses were performed on a CEM-focused microwave synthesis system in 20 mL vessels with septa at

90 Watts at 100 °C for 5 min. The absorbance measurements were realized on a FLUOstar Omega at 37 °C at 515 nm, taken every 90 s for 45 min.

### 3.1.1. General Procedure for the Synthesis of PPI-PhA and PPI-FA Generations 1, 2 and 3

In a double-necked round-bottomed flask, phloretic acid (ferulic acid) (1.05 eq/ $\text{NH}_2$ ) and the dendrimer PPI-n (1 eq) were dissolved in methanol (20 mL). The reaction mixture was stirred at reflux (65 °C) for 5 h; then, methanol was evaporated under reduced pressure. The residue obtained thereby was then dissolved in water (20 mL) and extracted with ethyl acetate (20 mL). The aqueous phase was then washed twice with ethyl acetate ( $2 \times 50$  mL) to remove excess phloretic acid (ferulic acid) and then evaporated under reduced pressure. The yellow solid salts were obtained in quantitative yields of >97%.

#### Data for PPI-1-PhA:



$^1\text{H}$  NMR (500 MHz,  $\text{CD}_3\text{OD}$ ),  $\delta$  (ppm): 1.42–1.44 (4H, H1, m); 1.76–1.78 (8H, H4, m); 2.41–2.49 (12H, H7, H2, m); 2.54 (8H, H3, t,  $J = 6.98$  Hz); 2.82 (8H, H8, t,  $J = 7.42$  Hz); 2.91 (8H, H5, t,  $J = 7.24$  Hz); 6.71 (8H, H11, H13, d,  $J = 8.61$  Hz); 7.05 (8H, H10, H14, d,  $J = 8.61$  Hz).

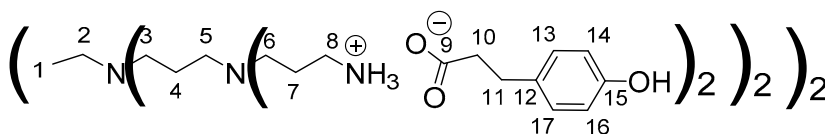
$^{13}\text{C}$  NMR (125 MHz,  $\text{CD}_3\text{OD}$ ),  $\delta$  (ppm): 24.0 (C1); 24.2 (C4); 31.4 (C8); 38.2 (C5); 39.8 (C7); 50.9 (C3); 53.2 (C2); 114.9 (C11, C13); 128.9 (C10, C14); 132.9 (C9); 155.1 (C12); 180.4 (C6).

IR ( $\text{cm}^{-1}$ ): 1540 ( $\nu\text{CO}_{\text{carboxylate}}$ , S), 1396 ( $\nu\text{CO}_{\text{carboxylate}}$ , S), 1210–1235 ( $\nu\text{C-O}_{\text{carboxylate}}$ , S).

Calculated elemental analysis of  $\text{C}_{52}\text{H}_{80}\text{N}_6\text{O}_{12}$ ,  $2\text{H}_2\text{O}$ : C: 61.4%; H: 8.32%; N: 8.26%; O: 22.02%.

Experimental elemental analysis of  $\text{C}_{52}\text{H}_{80}\text{N}_6\text{O}_{12}$ ,  $2\text{H}_2\text{O}$ : C: 61.79%; H: 8.56%; N: 8.58%; O: 21.06%.

#### Data for PPI-2-PhA:



$^1\text{H}$  NMR (500 MHz,  $\text{CD}_3\text{OD}$ ),  $\delta$  (ppm): 1.49–1.53 (4H, H1, m); 1.60–1.80 (24H, H4, H7, m); 2.39–2.69 (52H, H10, H2, H5, H3, H6, m); 2.80–2.83 (16H, H11, t,  $J = 7.42$  Hz); 2.88 (16H, H8, t,  $J = 7.85$  Hz); 6.70 (16H, H14, H16, d,  $J = 8.61$  Hz); 7.05 (16H, H13, H17, d,  $J = 8.61$  Hz).

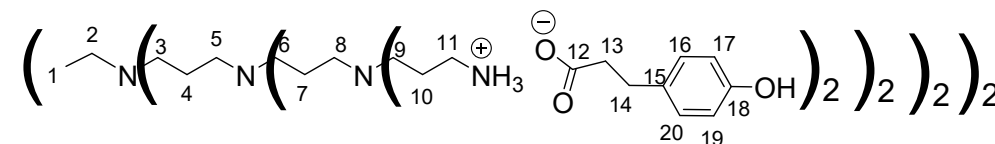
$^{13}\text{C}$  NMR (125 MHz,  $\text{CD}_3\text{OD}$ ),  $\delta$  (ppm): 22.41 (C4); 23.3 (C1); 24.6 (C7); 31.5 (C11); 38.1 (C8); 39.8 (C10); 50.7 (C6); 51.2 (C3); 51.3 (C5); 53.2 (C2); 114.8 (C14, C16); 128.9 (C13, C17); 132.9 (C12); 155.2 (C15); 180.5 (C9).

IR ( $\text{cm}^{-1}$ ): 1540 ( $\nu\text{CO}_{\text{carboxylate}}$ , S), 1396 ( $\nu\text{CO}_{\text{carboxylate}}$ , S), 1210–1235 ( $\nu\text{C-O}_{\text{carboxylate}}$ , S).

Calculated elemental analysis of  $\text{C}_{112}\text{H}_{176}\text{N}_{14}\text{O}_{24}$ ,  $5\text{H}_2\text{O}$ : C: 61.35%; H: 8.55%; N: 8.94%; O: 21.16%.

Experimental elemental analysis of  $\text{C}_{112}\text{H}_{176}\text{N}_{14}\text{O}_{24}$ ,  $5\text{H}_2\text{O}$ : C: 61.42%; H: 8.61%; N: 8.69%; O: 21.27%.

#### Data for PPI-3-PhA:



$^1\text{H}$  NMR (500 MHz,  $\text{CD}_3\text{OD}$ ),  $\delta$  (ppm): 1.43–1.47 (4H, H1, m); 1.58–1.80 (56H, H4, H7, H10, m); 2.30–2.68 (116H, H13, H2, H5, H8, H3, H6, H9, m); 2.76–2.97 (64H, H14, H11, m); 6.72 (32H, H17, H19, d,  $J = 8.5$  Hz); 7.05 (32H, H16, H20, d,  $J = 8.5$  Hz).

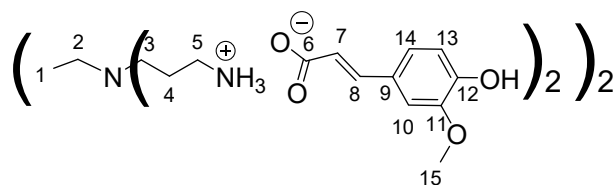
$^{13}\text{C}$  NMR (125 MHz,  $\text{CD}_3\text{OD}$ ),  $\delta$  (ppm): 22.4 (C4); 23.26 (C1); 24.6–24.6 (C7, C10); 31.5 (C14); 38.1 (C11); 39.8 (C13); 50.7 (C6, C9); 51.2 (C3); 51.3 (C5, C8); 53.2 (C2); 114.8 (C17, C19); 128.9 (C16, C20); 132.9 (C15); 155.2 (C18); 180.5 (C12)

IR ( $\text{cm}^{-1}$ ): 1540 ( $\nu\text{CO}_{\text{carboxylate}}$ , S), 1396 ( $\nu\text{CO}_{\text{carboxylate}}$ , S), 1210–1235 ( $\nu\text{C-O}_{\text{carboxylate}}$ , S).

Calculated elemental analysis of  $\text{C}_{232}\text{H}_{368}\text{N}_{30}\text{O}_{48}$ ,  $9\text{H}_2\text{O}$ : C: 61.82%; H: 8.63%; N: 9.32%; O: 20.23%.

Experimental elemental analysis of  $\text{C}_{232}\text{H}_{368}\text{N}_{30}\text{O}_{48}$ ,  $9\text{H}_2\text{O}$ : C: 62.14%; H: 8.62%; N: 9.32%; O: 20.40%.

Data for PPI-1-FA:



$^1\text{H}$  NMR (500 MHz,  $\text{CD}_3\text{OD}$ ),  $\delta$  (ppm): 1.31–1.33 (4H, H1, m); 1.76–1.80 (8H, H4, m); 2.43–2.45 (4H, H2, m); 2.54 (8H, H3, t,  $J = 7.35$  Hz); 2.98 (8H, H5, t,  $J = 7.35$  Hz); 3.86 (12H, H15, s); 6.36 (4H, H7, d,  $J = 15.82$  Hz); 6.82 (4H, H13, d,  $J = 8.11$  Hz); 6.98 (4H, H14, dd,  $J = 1.90$  Hz and  $J = 8.11$  Hz); 7.09 (4H, H10, d,  $J = 1.90$  Hz); 7.35 (4H, H8, d,  $J = 15.82$  Hz).

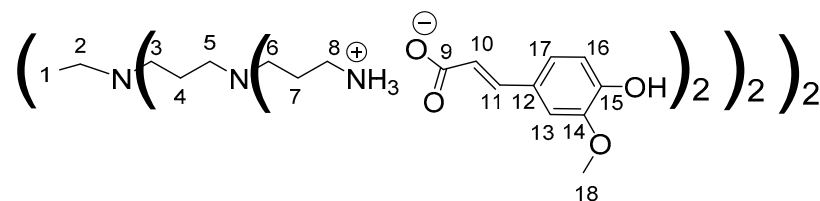
$^{13}\text{C}$  RMN (125 MHz,  $\text{CD}_3\text{OD}$ ),  $\delta$  (ppm): 24.1 (C1); 24.8 (C4); 38.4 (C5); 51.0 (C3); 53.2 (C2); 55.0 (C15); 109.9 (C10); 115.0 (C13); 121.4 (C14); 121.8 (C7); 127.7 (C9); 140.3 (C8); 147.9 (C11); 147.9 (C12); 174.7 (C6).

IR ( $\text{cm}^{-1}$ ): 1634 ( $\nu\text{CO}_{\text{carboxylate}}$ , S), 1372 ( $\nu\text{CO}_{\text{carboxylate}}$ , S), 1211 ( $\nu\text{C-O}_{\text{carboxylate}}$ , S).

Calculated elemental analysis of  $\text{C}_{56}\text{H}_{84}\text{N}_6\text{O}_{16}$ ,  $2\text{H}_2\text{O}$ : C: 59.56%; H: 7.50%; N: 7.40%; O: 25.5%.

Experimental elemental analysis of  $\text{C}_{56}\text{H}_{84}\text{N}_6\text{O}_{16}$ ,  $2\text{H}_2\text{O}$ : C: 58.80%; H: 7.77%; N: 8.08%; O: 25.34%.

Data for PPI-2-FA:



$^1\text{H}$  NMR (500 MHz,  $\text{CD}_3\text{OD}$ ),  $\delta$  (ppm): 1.40–1.43 (4H, H1, m); 1.59–1.62 (8H, H4, m); 1.79 (16H, H7, m); 2.32–2.67 (36H, H2, H5, H3, H6, m); 2.94 (16H, H8, t,  $J = 7.08$  Hz); 3.85 (24H, H18, s); 6.36 (8H, H10, d,  $J = 15.8$  Hz); 6.81 (8H, H16, d,  $J = 8.13$  Hz); 6.98 (8H, H17, dd,  $J = 8.13$  Hz,  $J = 1.91$  Hz); 7.09 (8H, H13, d,  $J = 1.91$  Hz); 7.35 (8H, H11, d,  $J = 15.8$  Hz).

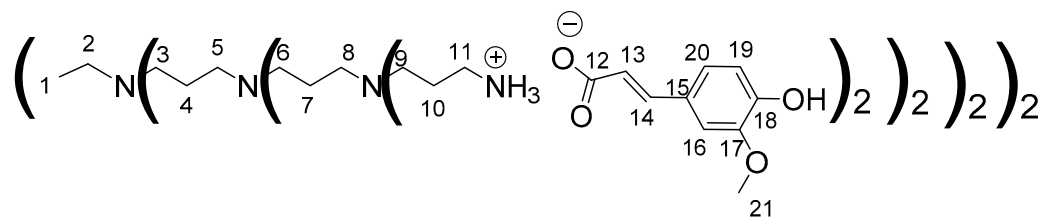
$^{13}\text{C}$  NMR (125 MHz,  $\text{CD}_3\text{OD}$ ),  $\delta$  (ppm): 22.4 (C4); 23.2 (C1); 24.6 (C7); 38.2 (C8); 50.8 (C6); 51.1 (C3); 51.2 (C5); 53.2 (C2); 55.1 (C18); 109.9 (C13); 115.3 (C16); 121.5 (C17); 121.9 (C10); 127.4 (C12); 140.3 (C11); 148.0 (C14); 148.3 (C15); 174.8 (C9).

IR ( $\text{cm}^{-1}$ ): 1635 ( $\nu\text{CO}_{\text{carboxylate}}$ , S), 1371 ( $\nu\text{CO}_{\text{carboxylate}}$ , S), 1211 ( $\nu\text{C-O}_{\text{carboxylate}}$ , S).

Calculated elemental analysis of  $\text{C}_{120}\text{H}_{176}\text{N}_{14}\text{O}_{32}$ ,  $5\text{H}_2\text{O}$ : C: 59.64%; H: 7.76%; N: 8.11%; O: 24.49%.

Experimental elemental analysis of  $\text{C}_{120}\text{H}_{176}\text{N}_{14}\text{O}_{32}$ ,  $5\text{H}_2\text{O}$ : C: 58.9%; H: 7.99%; N: 8.61%; O: 24.5%.

## Data for PPI-3-FA:



$^1\text{H}$  NMR (500 MHz,  $\text{CD}_3\text{OD}$ ),  $\delta$  (ppm): 1.42–1.46 (4H, H1, m); 1.50–1.81 (56H, H4, H7, H10, m); 2.27–2.62 (84H, H2, H5, H8, H3, H6, H9, m); 2.92–2.96 (32H, H11, m); 3.87 (48H, H21, s); 6.35 (16H, H13, d,  $J = 15.83$  Hz); 6.80 (16H, H19, d,  $J = 8.13$  Hz); 6.98 (16H, H20, dd,  $J = 1.9$  Hz and  $J = 8.13$  Hz); 7.10 (16H, H16, d,  $J = 1.9$  Hz); 7.34 (16H, H14, d,  $J = 15.83$  Hz).

$^{13}\text{C}$  NMR (125 MHz,  $\text{CD}_3\text{OD}$ ),  $\delta$  (ppm): 18.5 (C7); 22.9 (C4); 24.8 (C1, C10); 38.3 (C11); 50.8 (C6, C9, C3); 51.2 (C8, C5, C2); 55.1 (C21); 109.9 (C16); 115.3 (C19); 121.5 (C20); 121.9 (C13); 127.4 (C15); 140.2 (C14); 148.1 (C17); 148.1 (C18); 174.6 (C12).

IR ( $\text{cm}^{-1}$ ): 1635 ( $\nu\text{CO}_{\text{carboxylate}}$ , S), 1373 ( $\nu\text{CO}_{\text{carboxylate}}$ , S), 1211 ( $\nu\text{C-O}_{\text{carboxylate}}$ , S).

Calculated elemental analysis of  $\text{C}_{248}\text{H}_{368}\text{N}_{30}\text{O}_{64}$ ,  $13\text{H}_2\text{O}$ : C: 59.24%; H: 7.9%; N: 8.36%; O: 24.5%.

Experimental elemental analysis of  $\text{C}_{248}\text{H}_{368}\text{N}_{30}\text{O}_{64}$ ,  $13\text{H}_2\text{O}$ : C: 58.88%; H: 8.05%; N: 8.87%; O: 24.2%.

### 3.1.2. General Procedure for the Microwave-Assisted Synthesis of PPI-PhA and PPI-FA Generations 1, 2 and 3

Phloretic acid (ferulic acid) (1.05 eq/ $\text{NH}_2$ ) and PPI-*n* dendrimer (1 eq), dissolved in methanol (7 mL), were introduced to a CEM microwave oven; the mixture was heated at 100 °C for 5 min at a maximal power of 90 W. The mixture was then transferred to a flask and methanol was evaporated under reduced pressure. The residue obtained thereby was then dissolved in water (20 mL) and extraction with ethyl acetate (20 mL) was performed. The aqueous phase was then washed twice with ethyl acetate ( $2 \times 50$  mL) to remove excess phloretic acid (ferulic acid) and evaporated under reduced pressure. The yellow solid salts were obtained with quantitative yields of >98%.

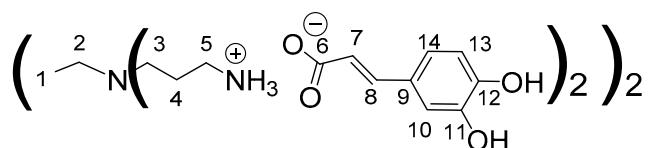
### 3.1.3. General Procedure for the Flow Synthesis of Ionic Dendrimers

A mixture containing 2.0 g of PPI, the adequate number of carboxylic acid (1 eq/ $\text{NH}_2$ ) and methanol (33.3 g) was prepared in a flask and stirred at room temperature for about 1 min until a homogeneous liquid was obtained. The mixture was then pumped into the Ehrfeld MMRS system at 0.24 mL/min using a Knauer Azura P4.15 HPLC pump. The flow reactor is represented in Scheme 3 and consists of a FlowPlate lab with a process plate LL, an insulation module and a backpressure regulator (Bronkhorst EL-Press). The temperature was settled to 150 °C using a Pilot One Ministat 230; a pressure of 3.5 bars was maintained via the BPR to prevent the evaporation of the medium. The residence time was confirmed by weighting the mixture obtained for a set amount of time (20 min). Each sample was then evaporated under vacuum at 45 °C, dissolved in methanol, washed three times with pentane/ethyl acetate (7/3) and dried under vacuum to obtain yellowish solids.

### 3.1.4. General Procedure for the Synthesis of PPI-CA Generations 1, 2 and 3

Caffeic acid (1.1 eq/ $\text{NH}_2$ ), dissolved in the ethanol (15 mL), was added dropwise in a round-bottomed flask containing the PPI-*n* dendrimer (1 eq.) dissolved in ethanol (10 mL). The reaction mixture was stirred at room temperature for 2 h using orbital stirring. The mixture was transferred to a centrifuge tube; the precipitation was recovered and washed 3 times with ethanol ( $3 \times 30$  mL) to remove excess caffeic acid before being dried under reduced pressure. The yellow solid salts were obtained, with yields of 90%, 90% and 92%, respectively, for generations 1, 2 and 3.

## Data for PPI-1-CA:



$^1\text{H}$  NMR (500 MHz,  $(\text{CD}_3)_2\text{SO}$ ),  $\delta$  (ppm): 1.30–1.34 (4H, H1, m); 1.60–1.64 (8H, H4, m); 2.27–2.30 (4H, H2, m); 2.37 (8H, H3, t,  $J = 6.87$  Hz); 2.73 (8H, H5, t,  $J = 7.26$  Hz); 6.14 (4H, H7, d,  $J = 15.76$  Hz); 6.69 (4H, H13, d,  $J = 8.08$  Hz); 6.80 (4H, H14, dd,  $J = 2.04$  Hz and  $J = 8.08$  Hz); 7.00 (4H, H10, d,  $J = 2.04$  Hz); 7.13 (4H, H8, d,  $J = 15.76$  Hz).

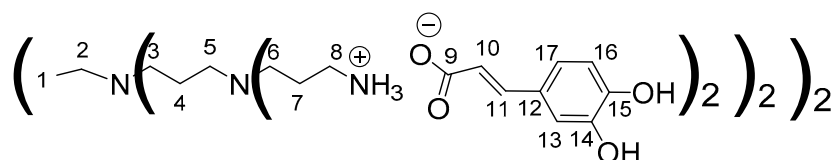
$^{13}\text{C}$  NMR (125 MHz,  $(\text{CD}_3)_2\text{SO}$ ),  $\delta$  (ppm): 24.9 (C1); 26.9 (C4); 38.6 (C5); 51.4 (C3); 53.6 (C2); 114.7 (C10); 116.3 (C13); 120.3 (C14); 122.4 (C7); 127.3 (C9); 140.1 (C8); 146.4 (C11); 147.9 (C12); 171.6 (C6).

IR ( $\text{cm}^{-1}$ ): 1504–1600 ( $\nu_{\text{CO}}$  carboxylate, S), 1375 ( $\nu_{\text{CO}}$  carboxylate, S), 1204–1230 ( $\nu_{\text{C-O}}$  carboxylate, S).

Calculated elemental analysis of  $\text{C}_{52}\text{H}_{72}\text{N}_6\text{O}_{16}$ ,  $2\text{H}_2\text{O}$ : C: 58.2%; H: 7.14%; N: 7.83%; O: 26.83%.

Experimental elemental analysis of  $\text{C}_{52}\text{H}_{72}\text{N}_6\text{O}_{16}$ ,  $2\text{H}_2\text{O}$ : C: 57.4%; H: 7.46%; N: 8.55%; O: 26.59%.

## Data for PPI-2-CA:



$^1\text{H}$  NMR (500 MHz,  $(\text{CD}_3)_2\text{SO}$ ),  $\delta$  (ppm): 1.27–1; 32 (4H, H1, m); 1.39–1.44 (8H, H4, m); 1.59–1.63 (16H, H7, m); 2.2–2.41 (36H, H2, H5, H3, H6, m); 2.74 (16H, H8, t,  $J = 6.95$  Hz); 6.15 (8H, H10, d,  $J = 15.76$  Hz); 6.71 (8H, H16, d,  $J = 8.09$  Hz); 6.85 (8H, H17, dd,  $J = 8.09$  Hz and  $J = 1.95$  Hz); 7.00 (8H, H13, d,  $J = 1.95$  Hz); 7.23 (8H, H11, d,  $J = 15.76$  Hz).

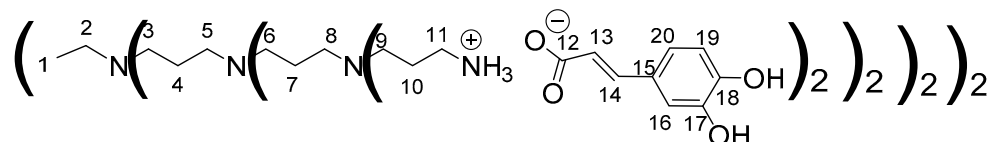
$^{13}\text{C}$  NMR (125 MHz,  $(\text{CD}_3)_2\text{SO}$ ),  $\delta$  (ppm): 24.8 (C1); 26.8 (C4); 27.1 (C7); 38.6 (C8); 49.9 (C6); 50.1 (C3); 51.3 (C5); 53.1 (C2); 109.1 (C13); 114.8 (C16); 116.3 (C17); 120.7 (C10); 126.9 (C12); 141.9 (C11); 146.3 (C14); 148.2 (C15); 171.6 (C9).

IR ( $\text{cm}^{-1}$ ): 1504–1600 ( $\nu_{\text{CO}}$  carboxylate, S), 1375 ( $\nu_{\text{CO}}$  carboxylate, S), 1204–1230 ( $\nu_{\text{C-O}}$  carboxylate, S).

Calculated elemental analysis of  $\text{C}_{112}\text{H}_{160}\text{N}_{14}\text{O}_{32}$ ,  $5\text{H}_2\text{O}$ : C: 58.37%; H: 7.72%; N: 9.15%; O: 25.39%.

Experimental elemental analysis of  $\text{C}_{112}\text{H}_{160}\text{N}_{14}\text{O}_{32}$ ,  $5\text{H}_2\text{O}$ : C: 57.21%; H: 7.9%; N: 9.72%; O: 25.16%.

## Data for PPI-3-CA:



$^1\text{H}$  NMR (500 MHz,  $(\text{CD}_3)_2\text{SO}$ ),  $\delta$  (ppm): 1.25–1.73 (60H, H1, H4, H7, H10, m); 2.16–2.43 (84H, H2, H5, H8, H3, H6, H9, m); 2.74 (32H, H11, m); 6.15 (16H, H13, d,  $J = 15.75$  Hz); 6.73 (16H, H19, d,  $J = 8.14$  Hz); 6.87 (16H, H20, d,  $J = 8.14$  Hz); 7.01 (16H, H16, s); 7.27 (16H, H14, d,  $J = 15.75$  Hz).

$^{13}\text{C}$  NMR (125 MHz,  $(\text{CD}_3)_2\text{SO}$ ),  $\delta$  (ppm): 24.8 (C1); 26.1 (C4); 27.0 (C7, C10); 38.6 (C11); 49.8 (C6, C9, C3); 51.3 (C8, C5, C2); 111.7 (C16); 114.9 (C19); 116.2 (C20); 120.9 (C13); 126.7 (C15); 140.2 (C14); 146.4 (C17); 148.0 (C18); 170.7 (C12).

IR ( $\text{cm}^{-1}$ ): 1504–1600 ( $\nu_{\text{CO}}$  carboxylate, S), 1375 ( $\nu_{\text{CO}}$  carboxylate, S), 1204–1230 ( $\nu_{\text{C-O}}$  carboxylate, S).

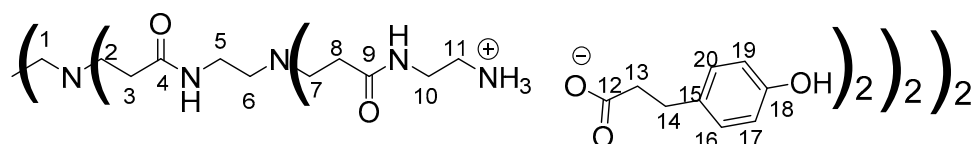
Calculated elemental analysis of  $C_{196}H_{316}N_{30}O_{54} \cdot 7H_2O$ : C: 57.66%; H: 8.15%; N: 10.29%; O: 23.9%.

Experimental elemental analysis of  $C_{196}H_{316}N_{30}O_{54} \cdot 7H_2O$ : C: 57.05%; H: 8.26%; N: 10.75%; O: 23.94%.

### 3.1.5. General Procedure for the Synthesis of PAMAM-PhA and PAMAM-FA Generations 1, 2 and 3

Phloretic acid (ferulic acid) (1.5 equiv. per  $NH_2$ ) and PAMAM-n dendrimer (1 equiv.), dissolved in methanol (20 mL), were introduced to a double-necked round-bottomed flask. The mixture was stirred at reflux (65 °C) for 16 h and the methanol was evaporated under reduced pressure. The residue obtained thereby was then dissolved in water (20 mL) and extracted with ethyl acetate (20 mL). The aqueous phase was then washed twice with ethyl acetate (2 × 50 mL) to remove the excess phloretic acid (ferulic acid). After evaporation, the yellow solid salts were obtained, with quantitative yields of >98%.

#### Data for PAMAM-1-PhA:



$^1H$  NMR (500 MHz,  $CD_3OD$ ),  $\delta$  (ppm): 2.29–2.49 (40H, H3, H8, H13, m); 2.5–2.61 (12H, H1, H6, m); 2.64–2.95 (40H, H2, H7, H14, m); 2.97–3.1 (16H, H11, m); 3.26 (8H, H5, m); 3.47–3.49 (16H, H10, m); 6.72 (16H, H16, H20, d,  $J = 8.46$  Hz) 7.05 (16H, H17, H19, d,  $J = 8.46$  Hz).

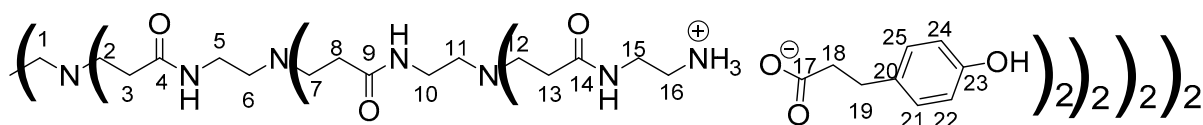
$^{13}C$  NMR (125 MHz,  $CD_3OD$ ),  $\delta$  (ppm): 31.5 (C14); 33.1 (C3, C8); 37.3 (C5, C10); 39.3 (C11); 39.8 (C13); 49.5 (C2, C7); 52.0 (C1, C6); 114.9 (C16, C20); 128.9 (C17, C19); 132.8 (C15); 155.1 (C18); 173.3 (C4); 174.4 (C9); 180.6 (C12).

IR ( $cm^{-1}$ ): 1540 ( $\nu_{CO}$  carboxylate, S), 1394 ( $\nu_{CO}$  carboxylate, S), 1211–1236 ( $\nu_{C-O}$  carboxylate, S).

Calculated elemental analysis of  $C_{134}H_{208}N_{26}O_{36} \cdot 13H_2O$ : C: 53.77%; H: 7.88%; N: 12.17%; O: 26.19%.

Experimental elemental analysis of  $C_{134}H_{208}N_{26}O_{36} \cdot 13H_2O$ : C: 54.1%; H: 8.32%; N: 11.34%; O: 26.23%.

#### Data for PAMAM-2-PhA:



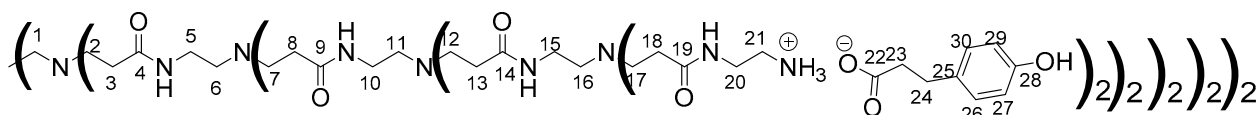
$^1H$  NMR (500 MHz,  $CD_3OD$ ),  $\delta$  (ppm): 2.29–2.50 (88H, H 3, H8, H13, H18, m); 2.51–2.63 (28H, H1, H6, H11, m); 2.67–2.92 (88H, H2, H7, H12, H19, m); 2.94–3.1 (32H, H16, m); 3.26 (24H, H5, H10, m); 3.38–3.48 (32H, H15, m); 6.72 (32H, H16, H20, d,  $J = 8.27$  Hz) 7.05 (32H, H17, H19, d,  $J = 8.27$  Hz);

$^{13}C$  NMR (125 MHz,  $CD_3OD$ ),  $\delta$  (ppm): 31.52 (C19); 33.1 (C3, C8, C13); 37.3 (C5, C10, C15); 39.3 (C16); 39.8 (C18); 49.5 (C2, C7, C12); 52.0 (C1, C6, C11); 114.9 (C21, C25); 128.9 (C22, C24); 132.8 (C20); 155.1 (C23); 173.3 (C4, C9); 174.4 (C14); 180.6 (C17).

IR ( $cm^{-1}$ ): 1540 ( $\nu_{CO}$  carboxylate, S), 1394 ( $\nu_{CO}$  carboxylate, S), 1211–1236 ( $\nu_{C-O}$  carboxylate, S).

Calculated elemental analysis of  $C_{286}H_{448}N_{58}O_{76} \cdot 32H_2O$ : C: 52.92%; H: 7.95%; N: 12.51%; O: 26.62%. Experimental elemental analysis of  $C_{286}H_{448}N_{58}O_{76} \cdot 32H_2O$ : C: 53.24%; H: 7.99%; N: 11.75%; O: 27.01%.

#### Data for PAMAM-3-PhA:



$^1\text{H}$  NMR (500 MHz,  $\text{CD}_3\text{OD}$ ),  $\delta$  (ppm): 2.25–2.49 (184H, H3, H8, H13, H18, H23, m); 2.50–2.62 (60H, H1, H6, H11, H16, m); 2.7–2.89 (184H, H2, H7, H12, H17, H24, m); 2.98–3.09 (64H, H21, m); 3.19–3.30 (56H, H5, H10, H15, m); 3.44 (64H, H20, m); 6.71 (64H, H26, H30, d,  $J = 8.3$  Hz); 7.05 (64H, H27, H29, d,  $J = 8.3$  Hz).

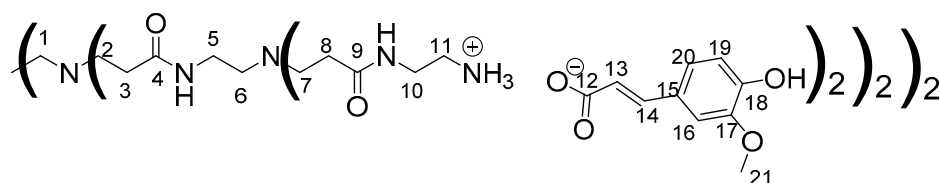
$^{13}\text{C}$  NMR (125 MHz,  $\text{CD}_3\text{OD}$ ),  $\delta$  (ppm): 31.5 (C24); 33.1 (C3, C8, C13); 33.3 (C18); 37.1–37.4 (C5, C10, C15, C20); 39.3 (C21); 39.8 (C23); 49.5 (C2, C7, C12, C17); 52.0 (C1, C6, C11, C16); 114.9 (C26, C30); 128.9 (C27, C29); 132.8 (C25); 155.1 (C28); 173.3 (C4, C9, C14); 174.4 (C19); 180.6 (C22).

IR ( $\text{cm}^{-1}$ ): 1540 ( $\nu\text{CO}_{\text{carboxylate}}$ , S), 1394 ( $\nu\text{CO}_{\text{carboxylate}}$ , S), 1211–1236 ( $\nu\text{C-O}_{\text{carboxylate}}$ , S).

Calculated elemental analysis of  $\text{C}_{590}\text{H}_{926}\text{N}_{122}\text{O}_{156}\cdot 98\text{H}_2\text{O}$ : C: 50.65%; H: 8.08%; N: 12.21%; O: 29.05%.

Experimental elemental analysis of  $\text{C}_{590}\text{H}_{926}\text{N}_{122}\text{O}_{156}\cdot 98\text{H}_2\text{O}$ : C: 51.04%; H: 8.00%; N: 11.40%; O: 29.04%.

#### Data for PAMAM-1-FA:



$^1\text{H}$  NMR (500 MHz,  $\text{CD}_3\text{OD}$ ),  $\delta$  (ppm): 2.29–2.43 (24H, H3, H8, m); 2.48–2.61 (12H, H1, H6, m); 2.64–2.87 (24H, H2, H7, m); 3–3.13 (16H, H11, m); 3.23 (8H, H5, m); 3.47 (16H, H10, m); 3.86 (24H, H21, s) 6,38 (8H, H13, d,  $J = 15.85$  Hz); 6.82 (8H, H19, d,  $J = 8.26$  Hz); 6,99(8H, H20, dd,  $J = 1.95$  Hz,  $J = 8.26$  Hz); 7.11 (8H, H16, d,  $J = 1.95$  Hz); 7.35 (8H, H14, d,  $J = 15.85$  Hz).

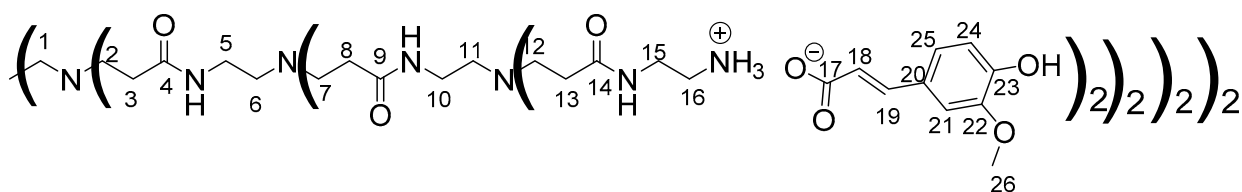
$^{13}\text{C}$  NMR (125 MHz,  $\text{CD}_3\text{OD}$ ),  $\delta$  (ppm): 33.2 (C3, C8); 37.2 (C5); 38.3 (C10); 39.7 (C11); 49.6 (C2, C7); 50.8 (C1); 52.0 (C6); 55.0 (C21); 109.9 (C16); 115.0 (C19); 121.5 (C13); 121.7 (C20); 127.7 (C15); 140.4 (C14); 147.9 (C17, C18); 173.2 (C4); 174.3 (C9); 174.6 (C12).

IR ( $\text{cm}^{-1}$ ): 1511–1590 ( $\nu\text{CO}_{\text{carboxylate}}$ , S), 1373 ( $\nu\text{CO}_{\text{carboxylate}}$ , S), 1220–1264 ( $\nu\text{C-O}_{\text{carboxylate}}$ , S).

Calculated elemental analysis of  $\text{C}_{142}\text{H}_{208}\text{N}_{26}\text{O}_{44}\cdot 16\text{H}_2\text{O}$ : C: 52.13%; H: 7.39%; N: 11.13%; O: 29.34%.

Experimental elemental analysis of  $\text{C}_{142}\text{H}_{208}\text{N}_{26}\text{O}_{44}\cdot 16\text{H}_2\text{O}$ : C: 52.21%; H: 7.79%; N: 11.13%; O: 28.87%.

#### Data for PAMAM-2-FA:



$^1\text{H}$  NMR (500 MHz,  $\text{CD}_3\text{OD}$ ),  $\delta$  (ppm): 2.20–2.46 (56H, H3, H8, H13, m); 2.48–2.60 (28H, H1, H6, H11, m); 2.66–2.92 (56H, H2, H7, H12, m); 3.00–3.16 (32H, H16, m); 3.23 (24H, H5, H10, m); 3.50 (32H, H15, m); 3.86 (48H, H26, s) 6.37 (16H, H18, d,  $J = 15.8$  Hz); 6.81 (16H, H24, d,  $J = 8.2$  Hz); 6.99 (16H, H25, dd,  $J = 1.95$  Hz,  $J = 8.2$  Hz); 7.11 (16H, H21, d,  $J = 1.95$  Hz); 7.35 (16H, H19, d,  $J = 15.8$  Hz).

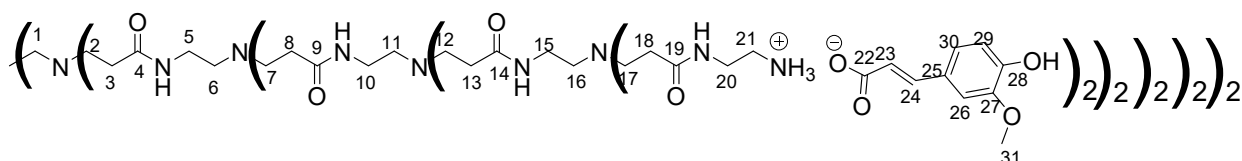
$^{13}\text{C}$  NMR (125 MHz,  $\text{CD}_3\text{OD}$ ),  $\delta$  (ppm): 33.2 (C3, C8, C13); 37.5 (C5, C10); 38.3 (C15); 39.7 (C16); 49.6 (C2, C7, C12); 51.0 (C1, C6, C11); 55.0 (C26); 109.9 (C21); 115.0 (C24); 121.5 (C18, C25); 127.7 (C20); 140.4 (C19); 147.9 (C22, C23); 174.2 (C4, C9, C14); 174.6 (C17).

IR ( $\text{cm}^{-1}$ ): 1511–1590 ( $\nu\text{CO}_{\text{carboxylate}}$ , S), 1373 ( $\nu\text{CO}_{\text{carboxylate}}$ , S), 1220–1264 ( $\nu\text{C-O}_{\text{carboxylate}}$ , S).

Calculated elemental analysis of  $\text{C}_{302}\text{H}_{448}\text{N}_{58}\text{O}_{92}\cdot 40\text{H}_2\text{O}$ : C: 51.21%; H: 7.51%; N: 11.47%; O: 29.81%.

Experimental elemental analysis of  $C_{302}H_{448}N_{58}O_{92} \cdot 40H_2O$ : C: 51.53%; H: 7.68%; N: 10.93%; O: 29.84%.

Data for PAMAM-3-FA:



$^1H$  NMR (500 MHz,  $CD_3OD$ ),  $\delta$  (ppm): 2.23–2.48 (120H, H3, H8, H13, H18, m); 2.47–2.61 (60H, H1, H6, H11, H16, m); 2.63–2.95 (120H, H2, H7, H12, H17, m); 3.02–3.17 (64H, H21, m); 3.17–3.28 (56H, H5, H10, H15, m); 3.40–3.56 (64H, H20, m); 3.86 (96H, H31, s); 6.37 (32H, H23, d,  $J = 15.8$  Hz); 6.82 (32H, H29, d,  $J = 8.27$  Hz); 6.99 (32H, H30, dd,  $J = 1.95$  Hz,  $J = 8.27$  Hz); 7.11 (32H, H26, d,  $J = 1.95$  Hz); 7.36 (32H, H24, d,  $J = 15.8$  Hz).

$^{13}C$  NMR (125 MHz,  $CD_3OD$ ),  $\delta$  (ppm): 33.2 (C3, C8, C13, C18); 37.17 (C5, C10, C15); 38.0 (C20); 39.6 (C21); 49.5 (C2, C7, C12, C17); 51.9 (C1, C6, C11, C16); 55.16 (C31); 110.0 (C26); 115.3 (C29); 121.5 (C30); 122.0 (C23); 127.6 (C25); 140.4 (C24); 148.0 (C27, C28); 174.4 (C4, C9, C14, C19); 174.9 (C22).

IR ( $cm^{-1}$ ): 1511–1590 ( $\nu CO_{\text{carboxylate}}$ , S), 1373 ( $\nu CO_{\text{carboxylate}}$ , S), 1220–1264 ( $\nu C-O_{\text{carboxylate}}$ , S).

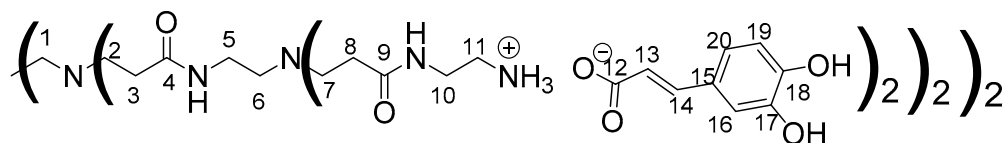
Calculated elemental analysis of  $C_{622}H_{928}N_{122}O_{188} \cdot 95H_2O$ : C: 50.36%; H: 7.60%; N: 11.52%; O: 30.52%.

Experimental elemental analysis of  $C_{622}H_{928}N_{122}O_{188} \cdot 95H_2O$ : C: 50.24%; H: 7.61%; N: 10.94%; O: 29.82%.

### 3.1.6. General Procedure for the Synthesis of PAMAM-CA Generations 1, 2 and 3

Caffeic acid (1.5 equiv. per  $NH_2$ ), dissolved in ethanol (15 mL), was introduced dropwise to a round-bottomed flask containing the PAMAM-*n* dendrimer (1 eq.), which had been previously dissolved in ethanol (10 mL). The reaction mixture was stirred at room temperature for 20 h using orbital stirring. The mixture was then transferred to a centrifuge. The residue recovered by filtration was then washed 3 times with ethanol ( $3 \times 30$  mL) to remove the excess caffeic acid. The product obtained thereby after evaporation under reduced pressure consisted of a white solid salt, with quantitative yields of >99% for generations 1 and 3 and 90% for generation 2.

Data for PAMAM-1-CA:



$^1H$  NMR (500 MHz,  $(CD_3)_2SO$ ),  $\delta$  (ppm): 2.14–2.99 (24H, H3, H8, m); 2.36–2.46 (12H, H1, H6, m); 2.56–2.7 (24H, H2, H7, m); 2.72–2.81 (16H, H11, m); 3.06–3.15 (8H, H5, m); 3.23 (16H, H10, m); 6.15 (8H, H13, d,  $J = 15.79$  Hz); 6.71 (8H, H19, d,  $J = 8.22$  Hz); 6.83 (8H, H20, dd,  $J = 2.08$  Hz,  $J = 8.22$  Hz); 6.98 (8H, H16, d,  $J = 2.08$  Hz); 7.20 (8H, H14, d,  $J = 15.79$  Hz).

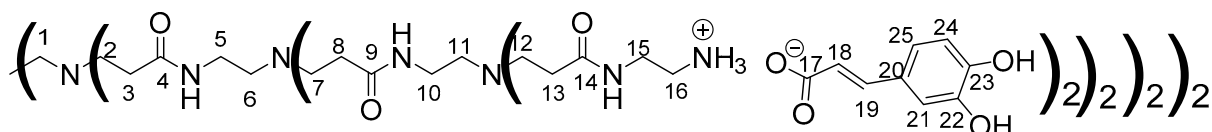
$^{13}C$  NMR (125 MHz,  $(CD_3)_2SO$ ),  $\delta$  (ppm): 33.8 (C3, C8); 37.4 (C5, C10); 39.0 (C11); 50.0 (C2, C7); 52.6 (C1, C6); 114.8 (C16); 116.3 (C19); 120.6 (C13); 121.0 (C20); 127.1 (C15); 141.1 (C14); 146.3 (C17); 148.0 (C18); 171.2 (C4, C9); 172.5 (C12).

IR ( $cm^{-1}$ ): 1522–1580 ( $\nu CO_{\text{carboxylate}}$ , S), 1376 ( $\nu CO_{\text{carboxylate}}$ , S), 1200–1220 ( $\nu C-O_{\text{carboxylate}}$ , S).

Calculated elemental analysis of  $C_{134}H_{192}N_{26}O_{44} \cdot 11H_2O$ : C: 52.44%; H: 7.03%; N: 11.87%; O: 28.67%.

Experimental elemental analysis of  $C_{134}H_{192}N_{26}O_{44} \cdot 11H_2O$ : C: 52.64%; H: 7.41%; N: 11.63%; O: 28.31%.

## Data for PAMAM-2-CA:



$^1\text{H}$  NMR (500 MHz,  $(\text{CD}_3)_2\text{SO}$ ),  $\delta$  (ppm): 2.02–2.29 (56H, H3, H8, H13, m); 2.34–2.47 (28H, H1, H6, H11, m); 2.56–2.79 (88H, H2, H7, H12, H15, m); 2.99–3.24 (56H, H5, H10, H15, m); 6.15 (13H, H18, d,  $J = 15.74$  Hz); 6.73 (13H, H24, d,  $J = 8.17$  Hz); 6.86 (13H, H25, dd,  $J = 2.14$  Hz,  $J = 8.17$  Hz); 6.98 (13H, H21, d,  $J = 2.14$  Hz); 7.26 (13H, H19, d,  $J = 15.74$  Hz).

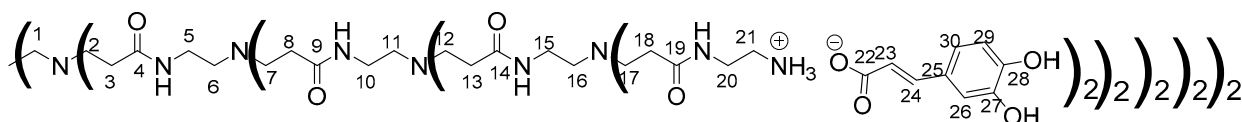
$^{13}\text{C}$  NMR (125 MHz,  $\text{CD}_3\text{OD}$ ),  $\delta$  (ppm): 33.7 (C3, C8, C13); 37.4 (C5, C10, C15); 39.0 (C16); 50.0 (C2, C7, C12); 52.5 (C1, C6, C11); 114.7 (C21); 116.3 (C24); 120.6 (C23); 121.0 (C25); 127.0 (C18); 141.1 (C19); 146.2 (C22, C23); 171.2 (C4, C9, C14); 172.7 (C17).

IR ( $\text{cm}^{-1}$ ): 1522–1580 ( $\nu\text{CO}_{\text{carboxylate}}$ , S), 1376 ( $\nu\text{CO}_{\text{carboxylate}}$ , S), 1200–1220 ( $\nu\text{C-O}_{\text{carboxylate}}$ , S).

Calculated elemental analysis of  $\text{C}_{286}\text{H}_{416}\text{N}_{58}\text{O}_{92}\cdot 20\text{H}_2\text{O}$ : C: 52.86%; H: 7.07%; N: 12.50%; O: 27.57%.

Experimental elemental analysis of  $\text{C}_{286}\text{H}_{416}\text{N}_{58}\text{O}_{92}\cdot 20\text{H}_2\text{O}$ : C: 52.21%; H: 7.09%; N: 12.87%; O: 27.83%.

## Data for PAMAM-3-CA:



$^1\text{H}$  NMR (500 MHz,  $(\text{CD}_3)_2\text{SO}$ ),  $\delta$  (ppm): 2.10–2.34 (120H, H3, H8, H13, H18, m); 2.35–2.48 (60H, H1, H6, H11, H16, m); 2.55–2.87 (184H, H2, H7, H12, H17, H21, m); 2.95–3.33 (120H, H5, H10, H15, H20, m); 6.16 (32H, H23, d,  $J = 15.79$  Hz); 6.72 (32H, H29, d,  $J = 8.24$  Hz); 6.85 (32H, H30, dd,  $J = 2.03$  Hz, and  $J = 8.24$  Hz); 6.98 (32H, H26, d,  $J = 2.03$  Hz); 7.24 (32H, H24, d,  $J = 15.79$  Hz).

$^{13}\text{C}$  NMR (125 MHz,  $(\text{CD}_3)_2\text{SO}$ ),  $\delta$  (ppm): 33.8 (C3, C8, C13, C18); 37.4 (C5, C10, C15, C20); 39.1 (C21); 50.0 (C2, C7, C12, C17); 52.6 (C1, C6, C11, C16); 114.8 (C26); 116.4 (C29); 120.6 (C23); 121.1 (C30); 127.1 (C25); 141.1 (C24); 146.3 (C27, C28); 171.2 (C4, C9, C14, C19); 172.6 (C22).

IR ( $\text{cm}^{-1}$ ): 1522–1580 ( $\nu\text{CO}_{\text{carboxylate}}$ , S), 1376 ( $\nu\text{CO}_{\text{carboxylate}}$ , S), 1200–1220 ( $\nu\text{C-O}_{\text{carboxylate}}$ , S).

Calculated elemental analysis of  $\text{C}_{590}\text{H}_{863}\text{N}_{122}\text{O}_{188}\cdot 26\text{H}_2\text{O}$ : C: 53.92%; H: 7.02%; N: 13.00%; O: 26.05%.

Experimental elemental analysis of  $\text{C}_{590}\text{H}_{863}\text{N}_{122}\text{O}_{188}\cdot 26\text{H}_2\text{O}$ : C: 53.16%; H: 7.50%; N: 13.75%; O: 25.58%.

## 3.1.7. Antioxidant Activity Evaluation of Synthesized Dendrimers

In a volumetric flask, a solution of 2,2-diphenyl 1-picrylhydrazyl (DPPH•) at  $6 \times 10^{-4}$  mol/L was prepared (2.37 mg in 25 mL of methanol). Then, a solution of the desired antioxidant ionic dendrimers was prepared, either in methanol for the phloretic and ferulic acid-based dendrimers or in a methanol/water/DMSO ((3:1:1)  $v/v/v$ ) mixture for the caffeic acid-based dendrimers. The solution was diluted to different concentrations in microplate wells. An equivalent volume of DPPH• solution (100  $\mu\text{L}$ /100  $\mu\text{L}$ ) was added to each well.

The absorbance measurements were realized using a FLUOstar Omega device at 515 nm every 90 s for 45 min to control the kinetics of the reaction. The curve of the percentage inhibition as a function of the concentrations ( $I$  (%) =  $f$  ([C])) gave the  $\text{IC}_{50}$  values (the concentration of the antioxidant necessary to inhibit 50% of DPPH) for each compound.

### 3.2. Cytotoxicity Experiment

#### 3.2.1. Cell Culture

Normal human dermal fibroblasts were purchased from Promocell (Heidelberg, Germany). They were grown in DMEM, supplemented with 10% fetal bovine serum (FBS) according to the manufacturer's specifications, in Nunclon® 75 cm<sup>2</sup> flasks (Dutscher Brumath, France) at 37 °C in a humid atmosphere containing 5% CO<sub>2</sub>.

#### 3.2.2. Cell Viability Assay

Cells were seeded in sterile 96-well microtiter plates (1 × 10,000 cells/well) and were allowed to settle for 24 h. Dendrimers were added to the cells at final concentrations of 0, 1, 10, 200, 500 and 1000 µg/mL in DMEM supplemented with 1% FBS. The cells were incubated for 48 h and imaged using an EVOS XL Core (Invitrogen) inverted microscope (×10 magnification) (Figure 5). Then, the medium was replaced by fresh medium containing 10% Wst-1 reagent. Absorbance was measured at 450 nm using a microplate spectrophotometer (SPECTROstar® Nano, BMG Labtech, Champigny-sur-Marne, France). Statistical analysis was performed using Student's *t*-test. The results are expressed as the mean ± standard deviation.

**Supplementary Materials:** The following supporting information can be downloaded at: <https://www.mdpi.com/article/10.3390/polym14173513/s1>, Figure S1: <sup>1</sup>H NMR of PPI-1-PhA in CD<sub>3</sub>OD; Figure S2: <sup>13</sup>C NMR of PPI-1-PhA in CD<sub>3</sub>OD; Figure S3: COSY NMR of PPI-1-PhA in CD<sub>3</sub>OD; Figure S4: HSQC NMR of PPI-1-PhA in CD<sub>3</sub>OD; Figure S5: HMBC NMR of PPI-1-PhA in CD<sub>3</sub>OD; Figure S6: <sup>1</sup>H NMR of PPI-2-PhA in CD<sub>3</sub>OD; Figure S7: <sup>13</sup>C NMR of PPI-2-PhA in CD<sub>3</sub>OD; Figure S8: <sup>1</sup>H NMR of PPI-3-PhA in CD<sub>3</sub>OD; Figure S9: <sup>1</sup>H NMR of PPI-1-FA in CD<sub>3</sub>OD; Figure S10: <sup>13</sup>C NMR of PPI-1-FA in CD<sub>3</sub>OD; Figure S11: COSY NMR of PPI-1-FA in CD<sub>3</sub>OD; Figure S12: HSQC NMR of PPI-1-FA in CD<sub>3</sub>OD; Figure S13: HMBC NMR of PPI-1-FA in CD<sub>3</sub>OD; Figure S14: <sup>1</sup>H NMR of PPI-2-FA in CD<sub>3</sub>OD; Figure S15: <sup>13</sup>C NMR of PPI-2-FA in CD<sub>3</sub>OD; Figure S16: <sup>1</sup>H NMR of PPI-3-FA in CD<sub>3</sub>OD; Figure S17: <sup>13</sup>C NMR of PPI-3-FA in CD<sub>3</sub>OD; Figure S18: IR of PPI-3-FA; Figure S19: <sup>1</sup>H NMR of PPI-1-CA in (CD<sub>3</sub>)<sub>2</sub>SO; Figure S20: <sup>13</sup>C NMR of PPI-1-CA in (CD<sub>3</sub>)<sub>2</sub>SO; Figure S21: <sup>1</sup>H NMR of PPI-2-CA in (CD<sub>3</sub>)<sub>2</sub>SO; Figure S22: <sup>13</sup>C NMR of PPI-2-CA in (CD<sub>3</sub>)<sub>2</sub>SO; Figure S23: <sup>1</sup>H NMR of PPI-3-CA in (CD<sub>3</sub>)<sub>2</sub>SO (weak solubility); Figure S24: <sup>13</sup>C NMR de PPI-3-CA in (CD<sub>3</sub>)<sub>2</sub>SO (weak solubility); Figure S25: IR of PPI-3-CA; Figure S26: IR of Caffeic acid; Figure S27: <sup>1</sup>H NMR of PAMAM-1-PhA in CD<sub>3</sub>OD; Figure S28: <sup>13</sup>C NMR of PAMAM-1-PhA in CD<sub>3</sub>OD; Figure S29: COSY NMR of PAMAM-1-PhA in CD<sub>3</sub>OD; Figure S30: IR of PAMAM-1-PhA; Figure S31: IR of Phloretic acid; Figure S32: <sup>1</sup>H NMR of PAMAM-2-PhA in CD<sub>3</sub>OD; Figure S33: IR of PAMAM-2-PhA; Figure S34: <sup>1</sup>H NMR of PAMAM-3-PhA in CD<sub>3</sub>OD; Figure S35: <sup>13</sup>C NMR of PAMAM-3-PhA in CD<sub>3</sub>OD; Figure S36: HMBC NMR of PAMAM-3-PhA in CD<sub>3</sub>OD; Figure S37: <sup>1</sup>H NMR of PAMAM-1-FA in CD<sub>3</sub>OD; Figure S38: <sup>13</sup>C NMR of PAMAM-1-FA in CD<sub>3</sub>OD; Figure S39: <sup>1</sup>H NMR of PAMAM-2-FA in CD<sub>3</sub>OD; Figure S40: IR of PAMAM-2-FA; Figure S41: <sup>1</sup>H NMR of PAMAM-1-CA in (CD<sub>3</sub>)<sub>2</sub>SO; Figure S42: <sup>13</sup>C NMR of PAMAM-1-CA in (CD<sub>3</sub>)<sub>2</sub>SO; Figure S43: IR of PAMAM-1-CA; Figure S44: <sup>1</sup>H NMR of PAMAM-2-CA in (CD<sub>3</sub>)<sub>2</sub>SO; Figure S45: IR of PAMAM-2-CA; Figure S46: <sup>1</sup>H NMR of PAMAM-3-CA in (CD<sub>3</sub>)<sub>2</sub>SO; Figure S47: IR of PAMAM-3-CA; IR of PAMAM-3-CA; Figure S48: Inhibition of DPPH (300 mol or 118.3 mg/L) by caffeic acid derived-PAMAM dendrimers; Figure S49: Inhibition of DPPH (300 mol or 118.3 mg/L) by ionic antioxidant dendrimers; Table S1: IC<sub>50</sub> (mg/L).

**Author Contributions:** Conceptualization, S.B., J.E. and M.D.; methodology, S.B., J.E. and M.D.; investigation, K.B., S.B.-P., J.-P.M., A.E.F., J.E. and C.C.; writing—original draft preparation, K.B., S.B.-P., S.B. and J.E.; writing—review and editing, K.B., S.B.-P., J.-P.M., S.B., A.E.F., J.E., C.C. and M.D.; supervision, S.B., J.E. and M.D.; project administration, S.B., J.E. and M.D.; funding acquisition, S.B., J.E. and M.D. All authors have read and agreed to the published version of the manuscript.

**Funding:** This research was co-funded by the European Research Development Fund and Wallonia in the scope of the France-Wallonie-Vlaanderen Interreg 2014–2020 program via the project InTiCosm (project number 1.1.338 INTICOSM).

**Institutional Review Board Statement:** Not applicable.

**Informed Consent Statement:** Not applicable.

**Data Availability Statement:** Not applicable.

**Acknowledgments:** All the authors are grateful to the Interreg France-Wallonie-Vlaanderen 2014–2020 Program (InTiCosm project, ERDF funding) for funding the research and KB PhD thesis. Universities of Reims Champagne-Ardenne (France) and Liège (Belgium) are acknowledged for support. K.B., S.B.-P., J.-P.M. and S.B. are grateful to Grand Est for co-funding the InTiCosm project. A.E.F., J.E., K.B., C.C. and M.D. are grateful to Wallonia for co-funding the InTiCosm project. M.D. thanks the F.R.S.-F.N.R.S. for her position as Senior Research Associate.

**Conflicts of Interest:** The authors declare no conflict of interest.

## References

1. Tomalia, D.A. The dendritic state. *Mater. Today* **2005**, *9*, 34–36.
2. Newkome, G.R.; Yao, Z.-Q.; Baker, G.R.; Gupta, V.K. Cascade molecules: A new approach to micelles. *J. Org. Chem.* **1985**, *9*, 2003–2004. [[CrossRef](#)]
3. Chis, A.A.; Dobrea, C.; Morgovan, C.; Arseniu, A.M.; Rus, L.L.; Butuca, A.; Juncan, A.M.; Totan, M.; Vonica-Tincu, A.L.; Cormos, G.; et al. Applications and Limitations of Dendrimers in Biomedicine. *Molecules* **2020**, *25*, 3982–4023. [[CrossRef](#)] [[PubMed](#)]
4. Kaur, D.; Jain, K.; Mehra, N.K.; Kesharwani, P.; Jain, N.K. A review on comparative study of PPI and PAMAM dendrimers. *J. Nanoparticle. Res.* **2016**, *146*, 18.
5. Menot, B.; Stopinski, J.; Martinez, A.; Oudart, J.B.; Maquart, F.X.; Bouquillon, S. Synthesis of surface-modified PAMAMs and PPIs for encapsulation purposes: Influence of the decoration on their sizes and toxicity. *Tetrahedron* **2015**, *71*, 3439. [[CrossRef](#)]
6. Mbakidi, J.P.; Barjhoux, I.; Aguib, K.; Geffard, A.; Rioult, D.; Palos Ladeiro, M.; Bouquillon, S. Synthesis of New Betaine-Based Ionic Liquids by Using a “One-Pot” Amidation Process and Evaluation of Their Ecotoxicity through a New Method Involving a Hemocyte-Based Bioassay. *ACS Sustain. Chem. Eng.* **2021**, *9*, 15427–15441. [[CrossRef](#)]
7. Maes, C.; Menot, B.; Hayouni, S.; Martinez, A.; Fauconnier, M.L.; Bouquillon, S. Preparation of new glycerol-based dendrimers and studies on their behavior towards essential oils encapsulation. *ACS. Omega* **2022**, *12*, 10277–10291. [[CrossRef](#)]
8. Schunk, T.; Hirsch, A. Dendritic Architectures with Positively Charged Cores and Negatively Charged Shells. *Eur. J. Org. Chem.* **2012**, *6*, 1130–1137. [[CrossRef](#)]
9. Salamonczyk, G.M. A Fast and Convenient Synthesis of New Water-Soluble, Polyanionic Dendrimers. *Molecules* **2021**, *26*, 4754–4768. [[CrossRef](#)]
10. Qiu, Z.L.; Fang, L.F.; Shen, Y.J.; Yu, W.H.; Zhu, B.K.; Helix-Nielsen, C.; Zhang, W. Ionic Dendrimer Based Polyamide Membranes for Ion Separation. *ACS Nano* **2021**, *15*, 7522–7535. [[CrossRef](#)]
11. Lebherz, T.; Weldin, D.L.; Hintennach, A.; Buchmeiser, M.R. Synthesis of Ionic Dendrimers and Their Potential Use as Electrolytes for Lithium-Sulfur Batteries. *Macromol. Chem. Phys.* **2020**, *221*, 1900436–1900442. [[CrossRef](#)]
12. Concellon, A.; Hernandez-Ainsa, S.; Barbera, J.; Romero, P.; Serrano, J.L.; Marcos, M. Proton conductive ionic liquid crystalline poly(ethyleneimine) polymers functionalized with oxadiazole. *RSC Adv.* **2018**, *8*, 37700–37706. [[CrossRef](#)] [[PubMed](#)]
13. Hernandez-Ainsa, S.; Barbera, J.; Marcos, M.; Serrano, J.L. Liquid Crystalline Ionic Dendrimers Containing Luminescent Oxadiazole Moieties. *Macromolecules* **2012**, *45*, 1006–1015.
14. Hernandez-Ainsa, S.; Barbera, J.; Marcos, M.; Serrano, J.L. Effect of the Phobic Segregation between Fluorinated and Perhydrogenated Chains on the Supramolecular Organization in Ionic Aromatic Dendrimers. *Chem. Mater.* **2010**, *22*, 4762–4768. [[CrossRef](#)]
15. Li, C.; Wei, Y.; Shi, W.; Wang, J.; Wang, B. Antioxidant capacity and kinetics of dendritic hindered phenols using DPPH assay. *Prog. React. Kinet. Mech.* **2015**, *40*, 279–290. [[CrossRef](#)]
16. Pocovi-Martinez, S.; Kemmer-Jonas, U.; Perez-Prieto, J.; Frey, H.; Stiriba, S.E. Supramolecular Antioxidant Assemblies of Hyperbranched Polyglycerols and Phenols. *Macromol. Chem. Phys.* **2014**, *215*, 2311–2317. [[CrossRef](#)]
17. Lee, C.Y.; Sharma, A.; Cheong, J.E.; Nelson, J.L. Synthesis and antioxidant properties of dendritic polyphenols. *Bioorg. Med. Chem. Lett.* **2009**, *19*, 6326–6330. [[CrossRef](#)]
18. Abderrezak, A.; Bourassa, P.; Mandeville, J.S.; Sedaghat-Herati, R.; Tajmir-Riahi, H.A. Dendrimers bind antioxidant polyphenols and cisPlatin drug. *PLoS ONE* **2012**, *7*, e33102.
19. Li, C.Q.; Guo, S.Y.; Wang, J.; Shi, W.G.; Zhang, Z.Q.; Wang, P.X. Kinetics and structure-activity relationship of dendritic bridged hindered phenol antioxidants to protect styrene against free radical induced peroxidation. *Russ. J. Phys. Chem. A* **2017**, *91*, 2350–2360. [[CrossRef](#)]
20. Li, C.; Zhai, X.; Guo, S.; Li, H.; Sun, P.; Wang, H.; Wang, J. Antiradical Ability of Dendrimer-Bridged Hindered Phenol and Its Antioxidant Property in Polyolefin. *ChemistrySelect* **2017**, *2*, 7202–7209. [[CrossRef](#)]
21. Del Olmo, N.S.; Gonzalez, C.E.P.; Rojas, J.D.; Gomez, R.; Ortega, P.; Escarpa, A.; De la Mata, F.J. Antioxidant and antibacterial properties of carbosilane dendrimers functionalized with polyphenolic moieties. *Pharmaceutics* **2020**, *12*, 698–703. [[CrossRef](#)] [[PubMed](#)]
22. Mencia, G.; Del Olmo, N.S.; Munoz-Moreno, L.; Maroto-Diaz, M.; Gomez, R.; Ortega, P.; Jose Carmena, M.; Javier de la Mata, F. Polyphenolic carbosilane dendrimers as anticancer agents against prostate cancer. *New J. Chem.* **2016**, *40*, 10488–10497. [[CrossRef](#)]

23. Soto-Castro, D.; Santillan, R.; Guadarrama, P.; Farfan, N.; Gonzalez-Herrera, I.G.; Cruz-Mendez, A.C. PAMAM-dendrimer bearing 1,2-diphenylethyne core obtained by palladium-catalyzed coupling assisted by silver oxide: In vitro evaluation of antioxidant properties. *Monatsh. Chem.* **2016**, *147*, 1839–1847. [[CrossRef](#)]
24. Li, C.; Sun, P.; Yu, H.; Zhang, N.; Wang, J. Scavenging ability of dendritic PAMAM bridged hindered phenolic antioxidants towards DPPH and ROO free radicals. *RSC. Adv.* **2017**, *7*, 1869–1876. [[CrossRef](#)]
25. Wang, Y.; Shen, W.; Shi, X.; Fu, F.; Fan, Y.; Shen, W.; Cao, Y.; Zhang, Q.; Qi, R. Alpha-Tocopheryl Succinate-Conjugated G5 PAMAM Dendrimer Enables Effective Inhibition of Ulcerative Colitis. *Adv. Healthc. Mater.* **2017**, *6*, 1700276–1700286. [[CrossRef](#)] [[PubMed](#)]
26. Kannan, A.; Saravanan, V.; Rajakumar, P. Synthesis, Photophysical, Electrochemical Studies, and Antioxidant Properties of Fluorescein-Linked Glycodendrimers. *Asian J. Org. Chem.* **2016**, *5*, 1155–1163. [[CrossRef](#)]
27. Mierina, I.; Peipina, E.; Aispure, K.; Jure, M. 1st generation dendrimeric antioxidants containing Meldrum's acid moieties as surface groups. *New J. Chem.* **2022**, *46*, 607–620. [[CrossRef](#)]
28. Balu, P.; Asharani, I.V.; Thirumalai, D. Synthesis of melamine core starburst polyamide G1 dendrimer and its antibacterial and antioxidant activities. *Asian J. Chem.* **2021**, *33*, 185–189. [[CrossRef](#)]
29. Savithri, J.S.; Rajakumar, P. Synthesis, Photophysical, and Antioxidant Properties of Rhodamine B Decorated Novel Dendrimers. *Aust. J. Chem.* **2018**, *71*, 399–406. [[CrossRef](#)]
30. Sathiyaraj, S.; Shanavas, A.; Kumar, K.A.; Sathiyaseelan, A.; Senthilselvan, J.; Kalaichelvan, P.T.; Nasar, A.S. The first example of bis(indolyl)methane based hyperbranched polyurethanes: Synthesis, solar cell application and anti-bacterial and anti-oxidant properties. *Eur. Polym. J.* **2017**, *95*, 216–231. [[CrossRef](#)]
31. Rajakumar, P.; Venkatesan, N.; Sekar, K.; Nagaraj, S.; Rengasamy, R. Synthesis, Optical, and Antioxidant Studies of Anthraquinone-core-based Dendrimers with NPhenylcarbazole as Surface Group. *Aust. J. Chem.* **2014**, *67*, 636–643. [[CrossRef](#)]
32. Rajakumar, P.; Venkatesan, N.; Sekar, K.; Nagaraj, S.; Rengasamy, R. Synthesis and antioxidant properties of enone core based dendrimers with carbazole as surface group. *Eur. J. Med. Chem.* **2010**, *45*, 1220–1224. [[CrossRef](#)] [[PubMed](#)]
33. Sowinska, M.; Morawiak, M.; Bochynska-Czyz, M.; Lipkowski, A.W.; Zieminska, E.; Zablocka, B.; Urbanczyk-Lipkowska, Z. Molecular antioxidant properties and in vitro cell toxicity of the p-aminobenzoic acid (PABA) functionalized peptide dendrimers. *Biomolecules* **2019**, *9*, 89–110. [[CrossRef](#)] [[PubMed](#)]
34. Mohamad Ali, B.; Velavan, B.; Sudhandiran, G.; Sridevi, J.; Sultan Nasar, A. Radical dendrimers: Synthesis, anti-tumor activity and enhanced cytoprotective performance of TEMPO free radical functionalized polyurethane dendrimers. *Eur. Polym. J.* **2020**, *122*, 109354–109359. [[CrossRef](#)]
35. Gallien, J.; Srinageshwar, B.; Gallo, K.; Holtgreffe, G.; Koneru, S.; Otero, P.S.; Bueno, C.A.; Mosher, J.; Roh, A.; Kohtz, D.S.; et al. Curcumin Loaded Dendrimers Specifically Reduce Viability of Glioblastoma Cell Lines. *Molecules* **2021**, *26*, 6050–6076. [[CrossRef](#)] [[PubMed](#)]
36. Falconieri, M.C.; Adamo, M.; Monasterolo, C.; Bergonzi, M.C.; Coronello, M.; Bilia, A.R. New Dendrimer-Based Nanoparticles Enhance Curcumin Solubility. *Planta Med.* **2017**, *83*, 420–425. [[CrossRef](#)]
37. Li, J.; Chen, L.; Xu, X.; Fan, Y.; Xue, X.; Shen, M.; Shi, X. Targeted Combination of Antioxidative and Anti-Inflammatory Therapy of Rheumatoid Arthritis using Multifunctional Dendrimer-Entrapped Gold Nanoparticles as a Platform. *Small* **2020**, *16*, e2005661. [[CrossRef](#)]
38. Zhang, D.; Huang, Q. Encapsulation of astragaloside with matrix metalloproteinase-2-responsive hyaluronic acid end-conjugated polyamidoamine dendrimers improves wound healing in diabetes. *J. Biomed. Nanotechnol.* **2020**, *16*, 1229–1240. [[CrossRef](#)]
39. Ambrosio, L.; Argenziano, M.; Cucci, M.A.; Grattarola, M.; De Graaf, I.A.M.; Dianzani, C.; Barrera, G.; Nieves, J.S.A.; Gomez, R.; Cavalli, R.; et al. Carbosilane dendrimers loaded with sirna targeting Nrf2 as a tool to overcome cisplatin chemoresistance in bladder cancer cells. *Antioxidants* **2020**, *9*, 993–1009. [[CrossRef](#)]
40. Sharma, R.; Kambhampati, S.P.; Zhang, Z.; Sharma, A.; Chen, S.; Duh, E.I.; Kannan, S.; Tso, M.O.M.; Kannan, R.M. Dendrimer mediated targeted delivery of sinomenine for the treatment of acute neuroinflammation in traumatic brain injury. *J. Control. Release* **2020**, *323*, 361–375. [[CrossRef](#)]
41. Sharma, R.; Kim, S.Y.; Sharma, A.; Zhang, Z.; Kambhampati, S.P.; Kannan, S.; Kannan, R.M. Activated microglia targeting dendrimer-minocycline conjugate as therapeutics for neuroinflammation. *Bioconjugate. Chem.* **2017**, *28*, 2874–2886. [[CrossRef](#)] [[PubMed](#)]
42. Alfei, S.; Marengo, B.; Zuccari, G.; Turrini, F.; Domenicotti, C. Dendrimer nanodevices and gallic acid as novel strategies to fight chemoresistance in neuroblastoma cells. *Nanomaterials* **2020**, *10*, 1243–1273. [[CrossRef](#)] [[PubMed](#)]
43. Alfei, S.; Catena, S.; Turrini, F. Biodegradable and biocompatible spherical dendrimer nanoparticles with a gallic acid shell and a double acting strong antioxidant activity as potential device to fight diseases from "oxidative stress". *Drug Deliv. Transl. Res.* **2020**, *10*, 259–270. [[CrossRef](#)] [[PubMed](#)]
44. Alfei, S.; Oliveri, P.; Malegori, C. Assessment of the Efficiency of a Nanospherical Gallic Acid Dendrimer for Long-Term Preservation of Essential Oils: An Integrated Chemometric-Assisted FTIR. *ChemistrySelect* **2019**, *4*, 8891–8901. [[CrossRef](#)]
45. Bi, J.; Li, Y.; Zhuang, Q.; Leng, Z.; Jia, H.; Liu, Y.; Zhou, J.; Du, L. Hydroxy-terminated poly(amidoamine) dendrimers as nanocarriers for the delivery of antioxidants. *J. Nanoparticle Res.* **2013**, *23*, 66–73. [[CrossRef](#)]

46. Sadeghi-Kiakhani, M.; Safapour, S.; Golpazir-Sorkheh, Y. Sustainable Antimicrobial and Antioxidant Finishing and Natural Dyeing Properties of Wool Yarn Treated with Chitosan-poly(amidoamine) Dendrimer Hybrid as a Biomordant. *J. Nat. Fibers* **2021**, 1–13. [[CrossRef](#)]
47. Shi, Y.; Ye, F.; Zhu, Y.; Miao, M. Development of dendrimer-like glucan-stabilized pickering emulsions incorporated with beta-carotene. *Food Chem.* **2022**, *385*, 132626. [[CrossRef](#)]
48. Shi, Y.; Ye, F.; Chen, Y.; Hui, Q.; Miao, M. Dendrimer-like glucan nanoparticulate system improves the solubility and cellular antioxidant activity of coenzyme Q10. *Food Chem.* **2020**, *333*, 127510–127518. [[CrossRef](#)]
49. Pentek, T.; Newenhouse, E.; O'Brien, B.; Chauhan, A.S. Development of a topical resveratrol formulation for commercial applications using dendrimer nanotechnology. *Molecules* **2017**, *22*, 137–153. [[CrossRef](#)]
50. Chanphai, P.; Tajmir-Riahi, H.A. Binding analysis of antioxidant polyphenols with PAMAM nanoparticles. *J. Biomol. Struct. Dyn.* **2018**, *36*, 3487–3495. [[CrossRef](#)]
51. De la Hoz, A.; Díaz-Ortiz, A.; Prieto, P. CHAPTER 1: Microwave-Assisted Green Organic Synthesis. *Altern. Energy Sources Green Chem.* **2016**, 1–33.
52. Hessel, V.; Escribà-Gelonch, M.; Bricout, J.; Nghiep Tran, N.; Anastasopoulou, A.; Ferlin, F.; Valentini, F.; Lanari, D.; Vaccaro, L. Quantitative sustainability assessment of flow chemistry—From simple metrics to holistic assessment. *ACS Sustain. Chem. Eng.* **2021**, *9*, 9508–9540. [[CrossRef](#)]
53. Stuerga, D. *Microwave-Material Interaction and Dielectric Properties, Key Ingredients for Mastery of Chemical Microwave Process in Microwave in Organic Synthesis*, 2nd ed.; Loupy, A., Ed.; Wiley-VCH: Weinheim, Germany, 2006; pp. 1–61.
54. Plusschack, M.B.; Pieber, P.; Gilmore, K.; Seeberger, P.H. The Hitchhiker's guide to flow chemistry. *Chem. Rev.* **2017**, *117*, 11796. [[CrossRef](#)] [[PubMed](#)]
55. Kar, S.; Sanderson, H.; Roy, K.; Benfenati, E.; Leszczynski, J. Green Chemistry in the synthesis of pharmaceuticals. *Chem. Rev.* **2022**, *122*, 3637–3710. [[CrossRef](#)]
56. Mohamad Aziz, N.A.; Yunus, R.; Kania, D.; Abd Hamid, H. Prospects and challenges of microwave-combined technology for biodiesel and biolubricant production through a transesterification: A review. *Molecules* **2021**, *26*, 788–809. [[CrossRef](#)]
57. Gérardy, R.; Debecker, D.P.; Estager, J.; Luis, P.; Monbaliu, J.-C.M. Continuous flow upgrading of selected C2–C6 platform chemicals derived from biomass. *Chem. Rev.* **2020**, *120*, 7219–7347. [[CrossRef](#)]
58. Bosman, A.W.; Janssen, H.M.; Meijer, E.W. About Dendrimers: Structure, Physical Properties, and Applications. *Chem. Rev.* **1999**, *99*, 1665–1688. [[CrossRef](#)]
59. Owen, R.W.; Haubner, R.; Mier, W.; Giacosa, A.; Hull, W.E.; Spiegelhalter, B.; Bartsch, H. Isolation, structure elucidation and antioxidant potential of the major phenolic and flavonoid compounds in brined olive drupes. *FCT* **2003**, *41*, 703–717. [[CrossRef](#)]
60. Bhat, F.M.; Riar, C.S. Extraction, identification and assessment of antioxidative compounds of bran extracts of traditional rice cultivars: An analytical approach. *Food Chem.* **2017**, *237*, 264–274. [[CrossRef](#)]
61. Rigoussen, A.; Verge, P.; Raquez, J.M.; Dubois, P. Direct Use of Natural Antioxidant-rich Agro-wastes as Thermal Stabilizer for Polymer: Processing and Recycling. *ACS Sustain. Chem. Eng.* **2018**, *6*, 13349–13357. [[CrossRef](#)]
62. Meghna, D.; Akshaya, G. Ferulic Acid: A natural essential compound having potential industrial and medicinal properties. *Int. J. Pharm. Sci.* **2022**, *13*, 603–611.
63. Zduńska, K.; Dana, A.; Kolodziejczak, A.; Rotsztein, H. Antioxidant Properties of Ferulic Acid and Its Possible Application. *Skin Pharmacol. Physiol.* **2018**, *31*, 332–336. [[CrossRef](#)] [[PubMed](#)]
64. Reitz, L.K.; Schroeder, J.; Longo, G.Z.; Boaventura, B.C.B.; Di Pietro, P.F. Dietary Antioxidant Capacity Promotes a Protective Effect against Exacerbated Oxidative Stress in Women Undergoing Adjuvant Treatment for Breast Cancer in a Prospective Study. *Nutrients* **2021**, *13*, 4234–4251. [[CrossRef](#)] [[PubMed](#)]
65. Swastika, M.; Manas, K.; Madhavan, N.; Devinder, A.; Sreedhara Ranganath, P.K.; Jayesh, R. Caffeic acid, a dietary polyphenol, as a promising candidate for combination therapy. *Chem. Pap.* **2022**, *76*, 1271–1283.
66. Prasad, N.; Jeyanthimala, K.; Ramachandran, S. Caffeic acid modulates ultraviolet radiation-B induced oxidative damage in human blood lymphocytes. *J. Photochem. Photobiol. B* **2009**, *95*, 196–203. [[CrossRef](#)]
67. Kang, N.J.; Lee, K.W.; Shin, B.J.; Jung, S.K.; Hwang, M.K.; Bode, A.M.; Heo, Y.S.; Lee, H.J.; Dong, Z. Caffeic acid, a phenolic phytochemical in coffee, directly inhibits Fyn kinase activity and UVB-induced COX-2 expression. *Carcinogenesis* **2009**, *30*, 321–330. [[CrossRef](#)]
68. Marcos, M.; Martin-Rapun, R.; Omenat, A.; Barbera, J.; Serrano, J.L. Ionic Liquid Crystal Dendrimers with Mono-, Di- and Trisubstituted Benzoic Acids. *Chem. Mater.* **2006**, *18*, 1206–1212. [[CrossRef](#)]
69. Dong, Z.; Wen, Z.; Zhao, F.; Kuhn, S.; Noël, T. Scale-up of micro- and milli-reactors: An overview of strategies, design principles and applications. *Chem. Eng. Sci. X* **2021**, *10*, 100097–100126. [[CrossRef](#)]
70. Glasnov, T.N.; Kappe, C.O. The microwave-to-flow paradigm: Translating high temperature batch microwave chemistry to scalable continuous-flow processes. *Chem. Eur. J.* **2011**, *17*, 11956–11968. [[CrossRef](#)]
71. Popovici, C.; Saykova, I.; Tylkowski, B. Evaluation de l'activité antioxydant des composés phénoliques par la réactivité avec le radical libre DPPH. *Rev. Génie Ind.* **2009**, *4*, 25–39.
72. Brand-Williams, W.; Cuvelier, M.E.; Berset, C. Use of a free radical method to evaluate antioxidant activity. *LWT Food Sci. Technol.* **1995**, *28*, 25–30. [[CrossRef](#)]

73. Pehlivan, F.E. *Vitamin C: An Antioxidant Agent*; Hamza, A.H., Ed.; IntechOpen: London, UK, 2017. Available online: <https://www.intechopen.com/chapters/56013> (accessed on 20 July 2022). [[CrossRef](#)]
74. Gómez Ruiz, B.; Roux, S.; Courtois, F.; Bonazzi, C. Spectrophotometric method for fast quantification of ascorbic acid and dehydroascorbic acid in simple matrix for kinetics measurements. *Food Chem.* **2016**, *211*, 583–589. [[CrossRef](#)] [[PubMed](#)]
75. Yáñez, E.; Santander, P.; Contreras, D.; Yáñez, J.; Cornejo, L.; Mansilla, L.D. Homogeneous and heterogeneous degradation of caffeic acid using photocatalysis driven by UVA and solar light. *J. Environ. Sci. Health Part A* **2016**, *51*, 78–85. [[CrossRef](#)] [[PubMed](#)]
76. Balieu, S.; Cadiou, C.; Martinez, A.; Nuzillard, J.M.; Oudart, J.B.; Maquart, F.X.; Chuburu, F.; Bouquillon, S. Encapsulation of contrast imaging agents by polypropyleneimine-based dendrimers. *J. Biomed. Mater. Res. Part A* **2013**, *101*, 613–621. [[CrossRef](#)] [[PubMed](#)]